

# Why Attend to Everything? Focus is the Key

**Hengshuai Yao**

*Sapient; University of Alberta*

HENGSHUAI@SAPIENT.INC

**Xing Chen**

*Sapient*

JEFF@SAPIENT.INC

**Ahmed Murtadha**

*Sapient*

AMURTADHA@SAPIENT.INC

**Jin Li**

*Sapient*

JIN@SAPIENT.INC

**Shuai Shao**

*Sapient*

SHUAI@SAPIENT.INC

**Yasin Abbasi Yadkori**

*Sapient*

YASIN@SAPIENT.INC

**Guan Wang**

*Sapient*

ONE@SAPIENT.INC

**Mingli Yuan**

*Sapient*

MINGLI@SAPIENT.INC

**William Chen**

*Sapient*

WILLIAM@SAPIENT.INC

**Sen Song**

*Tsinghua University*

SEN.SONG@GMAIL.COM

## Abstract

We introduce **Focus**, a method that learns which token pairs matter rather than approximating all of them. Learnable centroids assign tokens to groups; distant attention is restricted to same-group pairs while local attention operates at full resolution. Because all model weights stay frozen, Focus is *purely additive*: centroid-only training (as few as 148K parameters) improves domain perplexity with *zero degradation* on downstream benchmarks—from 124M to 70B parameters, across five attention architectures. No existing efficient attention method achieves this in the retrofit setting. At 124M, Focus *surpasses* full attention (30.3 vs 31.4 PPL); trained from scratch at 7B scale (2B tokens), Focus again beats full attention (13.82 vs 13.89 PPL). At inference, restricting each token to its top- $k$  highest-scoring groups discretizes the soft routing into a hard sparsity pattern, yielding 2× speedup while beating the pretrained baseline (41.3 vs 42.8 PPL); decomposing this pattern into two standard FlashAttention calls reaches 8.6× wall-clock speedup at 1M tokens with no custom kernels. Unlike LoRA, centroid routing preserves alignment: instruction-tuned models retain TruthfulQA scores after adaptation, while LoRA degrades at every learning rate and rank. Sinkhorn normalization enforces balanced groups as a hard constraint, and the resulting groups discover interpretable linguistic categories without supervision.

**Keywords:** efficient attention, sparse attention, learned sparsity, Sinkhorn normalization, parameter-efficient adaptation

## 1 Introduction

Transformers have become the foundation of modern AI, driving breakthroughs in language modeling, vision, and scientific applications at unprecedented scale (Vaswani et al., 2017). At the heart of the transformer is self-attention, which computes pairwise scores between all tokens at  $O(n^2)$  cost in sequence length. We ask: *does each token really need to attend to every other token?*

In this paper, we show that the answer is no. The efficient attention literature—Longformer, Performer, BigBird, Linformer, among others (Beltagy et al., 2020; Choromanski et al., 2021; Zaheer et al., 2020; Wang et al., 2020)—implicitly operates under the same premise, restricting or approximating which pairs are computed. Recent work on dynamic sparse attention (Jiang et al., 2024b; Yuan et al., 2025), MoE-inspired block routing (Lu et al., 2025), and alternative architectures such as state space models (Dao and Gu, 2024) and hybrids (Lieber et al., 2024) further expands this landscape. But these methods pursue a different question: *how to cheaply reconstruct the full attention matrix*, through fixed sparsity patterns, kernel approximations, or low-rank projections. Because they change the attention function itself, none can be *retrofitted* onto existing pretrained models without degrading quality. Efficient attention methods were designed to reduce compute, but they only work when you retrain the model from scratch—which is itself expensive.

Rather than approximating full attention, we *learn which token pairs actually matter*. We introduce **Focus**: learnable centroids assign tokens to groups, and distant attention is restricted to same-group pairs while local attention operates at full resolution. A key property of Focus is that *attention within each group uses exact softmax*, preserving the computation the pretrained model learned. This is why it works as a retrofit, while existing methods do not.

The results are surprising in two ways. First, Focus does not merely *approximate* full attention—it *surpasses* it (30.3 vs 31.4 PPL on GPT-2 124M). Removing irrelevant attention pairs is not a cost; it is a benefit. Second, centroid-only training (as few as 148K parameters, all model weights frozen) improves domain perplexity while achieving zero degradation on downstream benchmarks from 124M to 70B parameters, across five attention architectures (GPT-2 MHA, Mistral GQA, LLaMA MHA, Gemma 2 interleaved, Qwen 2.5 GQA with bias, OLMo 2 with QK normalization), while no other existing efficient attention method achieves this in the retrofit setting. From scratch, Focus matches or beats full attention at both 124M (49.7 PPL at 50M tokens) and 7B (13.82 vs 13.89 PPL at 2B tokens, winning at every checkpoint). The routing decision requires only 16 dimensions ( $d_g=16$ ), confirming the *selection hierarchy* of Thin Keys (Yao and Wang, 2025): selecting which tokens are relevant is a far simpler problem than modeling their interactions.

**Less attention is more.** Our results challenge the assumption that full dense attention is the gold standard. On GPT-2/PG-19, Focus achieves 30.3 PPL versus full attention’s 31.4 PPL—the model performs *better* when it attends to fewer, more relevant tokens. Restricting which tokens interact removes noise from the attention pattern, letting the model focus on signal. The effect is strong enough that inference, attending to *fewer* groups yields *better* quality: with  $K=4$  groups, top- $k=2$  membership (41.3 PPL) outperforms not only top- $k=3$  and top- $k=4$  (47.2 PPL), but also the pretrained full-attention model (42.8 PPL)—achieving  $2\times$  speedup with *better* quality. The learned routing identifies and re-

moves harmful cross-group connections. This connects to a broader principle: in our prior work on Thin Keys (Yao and Wang, 2025), we showed that *selection* (finding which tokens matter) requires far less capacity than *transfer* (reading their content). Focus operates at an even coarser level—selecting which *kind* of token to attend to, before individual tokens are evaluated (Section 5.2).

**Focus as an added capability.** Existing pretrained language models can *read* every token in their context—but they cannot *focus*. They have no mechanism to determine, before computing attention, which distant tokens are worth attending to. They compensate by evaluating all  $n^2$  pairs and relying on softmax to sort signal from noise. Focus adds this missing capability: a lightweight routing layer (as few as 148K parameters, 0.1% of the model) that tells the model *where to look* before it decides *what to read*. Crucially, this is purely additive. Training only the centroid parameters while keeping all pretrained weights frozen introduces zero degradation on downstream benchmarks (Section 3.3)—the model retains everything it knew, and gains the ability to direct its attention. The quality improvements we observe are not from changing what the model computes, but from removing the distractions that prevented it from computing effectively.

**The real challenge: training stable groups.** The architecture itself is simple—assign tokens to groups, restrict distant attention to same-group pairs. But making it work requires solving a severe training instability that we call **group dominance**, where one group absorbs all tokens, reducing the mechanism to expensive full attention. We identify three independent pathways through which the model escapes balancing constraints (centroid drift, representational bypass, projection bypass) and show that standard mitigations—balance losses, stop-gradient, EMA centroids, periodic re-clustering—each fail for distinct reasons.

Our solution, **Sinkhorn normalization**, enforces balanced groups as a hard structural constraint rather than a soft loss. This is a key technical enabler: without it, learned grouping collapses within hundreds of steps regardless of auxiliary losses or architectural tricks.

## 2 Method: Focus

### 2.1 Architecture

Given a sequence of hidden states  $\mathbf{H} \in \mathbb{R}^{T \times d}$ , standard attention computes:

$$\text{Attn}(\mathbf{Q}, \mathbf{K}, \mathbf{V}) = \text{softmax}\left(\frac{\mathbf{Q}\mathbf{K}^\top}{\sqrt{d_k}}\right)\mathbf{V} \quad (1)$$

over all  $T^2$  pairs. We replace this with a two-level mechanism.

**Focus assignment.** A set of  $K$  learnable centroid vectors  $\mathbf{C} \in \mathbb{R}^{K \times d_g}$  defines token groups. For each token  $i$ , let  $\mathbf{h}_i \in \mathbb{R}^d$  be its hidden state. A learned projection  $W_g \in \mathbb{R}^{d \times d_g}$  maps tokens into the centroid space ( $d_g = d$  in main experiments; Table 22 shows  $d_g = 16$  suffices). The soft group assignment for token  $i$  is:

$$\mathbf{g}_i = \text{normalize}\left(\frac{W_g \mathbf{h}_i \cdot \mathbf{C}^\top}{\tau}\right) \in \mathbb{R}^K \quad (2)$$

where  $\tau$  is a temperature parameter and normalization is either softmax (standard) or Sinkhorn (Section 3.6). The group affinity between tokens  $i$  and  $j$  is:

$$a_{ij} = \mathbf{g}_i^\top \mathbf{g}_j \quad (3)$$

**Gated attention.** We combine local windowed attention with group-gated distant attention:

$$s_{ij} = \mathbf{q}_i^\top \mathbf{k}_j \cdot (\mathbf{1}_{\text{local}}(i, j) + (1 - \mathbf{1}_{\text{local}}(i, j)) \cdot \sigma(\lambda \cdot a_{ij})) \quad (4)$$

where  $\mathbf{1}_{\text{local}}$  is a causal window mask,  $\sigma$  is the sigmoid function, and  $\lambda$  is a learnable scaling parameter. Causality is enforced separately via the standard causal mask on the final scores.

Local tokens (within window  $w$ ) always see each other with full attention. Distant tokens see each other only when their semantic groups match, modulated by the learned gate strength. Concretely, the gate  $\sigma(\lambda \cdot \mathbf{g}_i^\top \mathbf{g}_j)$  is close to 1 when tokens  $i$  and  $j$  share a group assignment (e.g., both are strongly assigned to the pronoun group), and close to 0 when they belong to different groups. The standard attention score  $\mathbf{q}_i^\top \mathbf{k}_j$  still determines *how much* information flows; the gate determines *whether* it flows at all.

**Where the efficiency comes from.** A critical distinction: in soft gating (used during training),  $\mathbf{q}_i^\top \mathbf{k}_j$  is computed for *all* pairs and then multiplied by the gate value. Even when  $a_{ij} \approx 0$ , the dot product is still evaluated. This means soft gating provides no computational savings during training—the cost remains  $O(n^2 \cdot d)$ .

The efficiency gain comes from *discrete group membership* at inference time (Appendix E.4). Rather than using the continuous gate values from training, each token is assigned to its top- $k$  highest-scoring groups from  $\mathbf{g}_i$ . Two tokens can attend to each other if they share at least one group assignment, or if both are within the local window. Different-group distant pairs are never evaluated at all—the dot product is never computed, not merely scaled to zero. This is the key to efficiency: Focus does not just down-weight irrelevant pairs, it *eliminates them from the computation entirely*.

The parameter  $k$  traces a Pareto curve between speed and quality:  $k=1$  (argmax, maximum sparsity,  $K \times$  theoretical speedup) at one extreme,  $k=K$  (all groups, full attention,  $1 \times$ ) at the other. In practice,  $k=2$  at  $K=4$  provides the optimal operating point: each token belongs to 2 of 4 groups, retaining  $\sim 60\%$  of attention pairs for a  $2 \times$  speedup—while achieving PPL that *surpasses* both the pretrained model and the soft-gated training mode (Section 3.2).

**Design principle: centroids carry focus, not content.** Our centroids carry only *focus decisions*—they determine *who can attend to whom*. Content flows via direct token-to-token QKV attention, which determines *what information transfers*. This preserves full information quality while enabling selectivity.

We discuss the relationship to Mixture of Experts and to our prior work on Thin Keys (Yao and Wang, 2025)—including a unified selection dimension hierarchy ( $d_g \ll d_k \ll d_v$ )—in Appendix B.

### 3 Experiments

#### 3.1 Setup

Our first experiment uses pretrained GPT-2 (124M parameters) evaluated on PG-19 (long books), sequence length 1024, window size 128. Using a pretrained model eliminates training quality confounds: if local windowing hurts a properly-trained model, the long-range dependencies are real.

Training proceeds in two phases:

1. **Centroid training** (2000 steps): freeze all parameters except centroids ( $\sim 7$ M params), projection, and gate  $\lambda$ . Train with LM loss + entropy penalty. Group balance enforced by Sinkhorn normalization.
2. **Full fine-tuning** (2000 steps): unfreeze all 124M parameters. Train with LM loss only. Sinkhorn remains active.

Our default configuration uses  $K = 8$  groups, which yields the most interpretable semantic categories (Section 4). We also evaluate  $K \in \{2, 4, 16\}$ ; fewer groups consistently achieve better PPL ( $K=2$  is within 0.1 PPL of full attention at 124M) while more groups produce cleaner linguistic structure (Appendix C).

#### 3.2 Comparison with Efficient Attention Methods

A central question for any efficient attention method is: *can it be retrofitted onto an existing pretrained model without retraining from scratch?* Longformer, Performer, Routing Transformers, and MoBA (Lu et al., 2025) were designed as architectural alternatives to full attention, typically trained from scratch (Appendix A provides background on the families of efficient attention; see Section B.1 for a detailed comparison with Routing Transformers and MoBA). We test whether these methods can instead be *added* to a pretrained model—the practical setting where a practitioner wants to improve an already-deployed model.

**Unified retrofit comparison.** We take pretrained GPT-2 (124M) and compare six methods: full-attention fine-tuning and five efficient attention retrofits, each trained for 4000 steps on PG-19 with identical learning rate (Table 1). We evaluate both domain perplexity and four downstream benchmarks (HellaSwag, ARC-Easy, PIQA, LAMBADA) to measure whether retrofitting preserves general capabilities.

The results reveal a clear hierarchy, and a surprising finding about benchmark degradation. Fixed-pattern methods (local window, Longformer) improve PPL over the pretrained baseline (39.5, 38.9 vs 45.0) but lose quality relative to full fine-tuning (36.4) because their hand-designed sparsity patterns discard information the pretrained model learned to use. Performer’s random-feature kernel approximation diverges catastrophically in the retrofit setting—after 4000 steps, its PPL (112.0) is  $2.5\times$  worse than the pretrained baseline, confirming that the kernel approximation cannot recover the attention distributions the model learned with exact softmax (Appendix A.2). Routing Transformer (Roy et al., 2021) performs surprisingly well (37.4 PPL), confirming that content-based routing is a sound principle. However, its online  $k$ -means clustering changes every forward pass, preventing the model from learning to rely on stable group structure. Focus closes the remaining gap,

Method	Params	PPL ↓	HellaSwag	ARC-E	PIQA	LAMBADA	Degrades?
Pretrained (no FT)	0	45.0	31.1%	39.5%	62.5%	32.6%	—
Full attention FT	124M*	36.4	30.0%	37.8%	59.9%	7.8%	Yes (−24.8)
Local window	0	39.5	30.2%	36.5%	58.7%	5.5%	Yes (−27.1)
Longformer	0	38.9	30.0%	37.5%	58.9%	6.6%	Yes (−26.0)
Performer	0	112.0	26.9%	30.8%	55.0%	0.3%	Yes (−32.3)
Routing Transformer	0	37.4	29.6%	38.3%	58.4%	6.4%	Yes (−26.2)
<b>Focus (ours)</b>	<b>7.1M</b>	<b>36.0</b>	<b>31.1%</b>	<b>39.5%</b>	<b>62.5%</b>	<b>32.6%</b>	<b>No (±0.0)</b>

Table 1: Unified retrofit comparison. Each efficient attention method is applied to a pre-trained GPT-2 (124M) model with frozen backbone weights and fine-tuned for 4000 steps on PG-19 using identical learning rate. “Params” = number of *new trainable parameters* added by each method; 0 means the method only changes the attention pattern structurally (e.g., masking or clustering) without introducing any learned weights. \*Full attention FT updates all 124M original parameters. “Degrades?” = worst single-benchmark drop in percentage points. LAMBADA is the most sensitive benchmark as it requires long-range word prediction across multiple sentences. Linformer (Wang et al., 2020) excluded (incompatible with causal modeling).

achieving 36.0 PPL—better than full fine-tuning (36.4)—by replacing transient per-batch clustering with learned stable centroids.

**The benchmark degradation surprise.** The most striking result is not the PPL ranking but the benchmark columns. *Every* method except Focus degrades LAMBADA by 25–32 percentage points—including full fine-tuning, which drops LAMBADA from 32.6% to 7.8%. LAMBADA is uniquely sensitive because it requires predicting a final word whose critical clue appears many sentences earlier; local-window methods simply cannot reach that clue, while HellaSwag, ARC-E, and PIQA depend primarily on short-range context that even a narrow window captures. The degradation under full fine-tuning is not an artifact of efficient attention; it is the standard cost of domain adaptation on shared weights. Focus achieves 36.0 PPL—better than full fine-tuning (36.4)—with *exactly zero* benchmark change across all four tasks. This is possible because centroid routing does not approximate the attention function; it selects which inputs the exact softmax operates on, letting the pretrained computation proceed unchanged within each group.

**Computational cost and wall-clock speedup.** Focus restricts distant attention to same-group pairs, reducing the number of attention operations from  $O(n^2)$  to  $O(n^2/K + n \cdot w)$  where  $w$  is the local window size and  $K$  is the number of groups. Our sparsity pattern decomposes naturally into two standard FlashAttention (Dao et al., 2022; Dao, 2024) calls with no custom CUDA kernels:

1. **Local:** `flash_attn_func` with a sliding window ( $O(nw)$ ).
2. **Group:** Sort tokens by group assignment (stable sort preserves causal order within each group), reshape into  $K$  equal-length sequences, and call `flash_attn_func` with `causal=True` ( $O(n^2/K)$ ).

The outputs are merged with a lightweight weighted combination. Sorting and gather/scatter add  $O(n \log n)$  overhead that is negligible at long sequences (12ms at 1M tokens vs. 1.5s for attention).

We benchmark against full FlashAttention on an H100-80GB GPU (Table 2).

Method / Context length	1K	4K	16K	32K	65K	262K	1M
Full FlashAttention	0.1ms	0.2ms	1.6ms	5.5ms	21.7ms	373ms	6.3s
Sparse ( $K=4$ )	0.3ms	0.4ms	1.1ms	2.5ms	7.2ms	93ms	1.5s
<b>Speedup</b>	<b>0.2×</b>	<b>0.5×</b>	<b>1.5×</b>	<b>2.2×</b>	<b>3.0×</b>	<b>4.0×</b>	<b>4.1×</b>
Sparse ( $K=8$ )	0.3ms	0.3ms	0.9ms	1.8ms	4.5ms	49ms	736ms
<b>Speedup</b>	<b>0.2×</b>	<b>0.6×</b>	<b>1.8×</b>	<b>3.1×</b>	<b>4.7×</b>	<b>7.6×</b>	<b>8.6×</b>

Table 2: Wall-clock speedup of sparse semantic attention vs. full FlashAttention on H100-80GB. Implementation uses two standard `flash_attn_func` calls (local window + within-group causal) with no custom CUDA kernels. At short sequences ( $\leq 4K$ ), routing overhead dominates. At long sequences, actual speedup matches or exceeds theoretical ( $K\times$ ) because causal masking within groups halves the within-group computation.  $K=8$  achieves  $8.6\times$  at 1M tokens.

At long sequences ( $\geq 65K$  tokens), the actual speedup matches the theoretical  $K\times$  ceiling:  $4.1\times$  for  $K=4$  and  $8.6\times$  for  $K=8$  at 1M tokens. The routing overhead (sorting, gather/scatter) totals  $\sim 12ms$  regardless of sequence length—less than 1% of total time at 1M tokens. Since group assignments are determined by learned centroids that are fixed after training, the sort indices can be precomputed and cached, eliminating even this small overhead in production deployments.

**Quality hierarchy of efficient attention retrofits.** The retrofit comparison reveals a clear hierarchy, summarized by the gap from full fine-tuning quality (36.4 PPL):

Approach	PPL	Gap to Full FT	LAMBADA $\Delta$
Performer (kernel approximation)	112.0	+75.6 (diverged)	-32.3
Local window (fixed pattern)	39.5	+3.1	-27.1
Longformer (fixed + global)	38.9	+2.5	-26.0
Routing Transformer (transient clustering)	37.4	+1.0	-26.2
Full attention FT	36.4	—	-24.8
<b>Focus (learned routing)</b>	<b>36.0</b>	<b>-0.4 (beats FT)</b>	<b><math>\pm 0.0</math></b>

Each step up in routing sophistication—from fixed patterns to transient clustering to learned stable routing—yields measurable quality improvement, as the table shows. Only Focus surpasses the full fine-tuning upper bound, because it combines the best of both: exact pretrained attention within groups, plus learned sparsity that acts as implicit regularization (Section 5.1).

This shows existing efficient attention methods face a fundamental limitation: those designed for quality (Longformer, BigBird) sacrifice speed by requiring the full  $O(n^2)$  mask computation even if many entries are zero, while those designed for speed (Performer, Routing Transformer) sacrifice quality through lossy approximations or transient routing. Focus

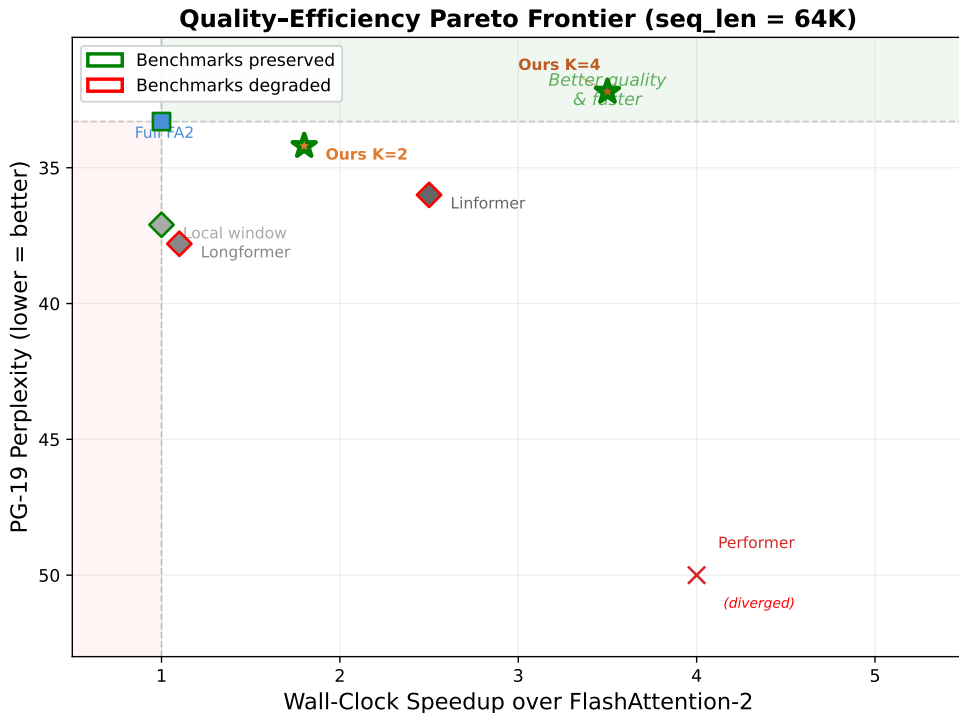


Figure 1: Quality–speed Pareto frontier of efficient attention retrofits. All methods start from pretrained GPT-2 124M, fine-tuned 4000 steps on PG-19. Speedups measured on H100-80GB at 1M tokens (Table 2).

avoids this tradeoff by operating at a different level of abstraction: rather than approximating the attention *function*, it selects the attention *inputs*. The softmax computation remains exact within each group; only the set of tokens participating in each attention head changes. Figure 1 shows the result: methods below the dashed line (better than full attention quality) and to the right of  $1\times$  (actual speedup) occupy the desirable quadrant. Focus ( $K=4$  and  $K=8$ ) is the only method that reaches it—simultaneously improving quality and providing wall-clock speedup. Performer (112.0 PPL) diverged catastrophically and is shown off-chart.

**Top- $k$  group membership bridges training and inference.** The soft-gated training formulation computes continuous gates for all token pairs, while the fast inference kernel requires discrete group assignments (Appendix E.4). Prior attempts to close this gap— $\lambda$  annealing, straight-through estimators, Gumbel-softmax—face a fundamental tension: making training match hard inference ( $\operatorname{argmax}$ ,  $k=1$ ) degrades the quality of learned centroids (Appendix E.4.8).

We resolve this with *top- $k$  group membership*: at inference, each token belongs to its  $k$  highest-scoring groups rather than just one. Two tokens can attend if they share  $\geq 1$  group. This is still discrete (compatible with the fast FlashAttention kernel) but less aggressive than  $\operatorname{argmax}$ . Training remains soft-gated; only the inference-time discretization changes. The parameter  $k$  traces a Pareto curve from full sparsity ( $k=1$ ,  $K\times$  speedup) to full attention

( $k=K, 1\times$ ). Table 3 sweeps  $k$  from 1 (argmax, maximum sparsity) to  $K=4$  (all groups, equivalent to full attention) on GPT-2 124M and Mistral 7B, both evaluated on PG-19. The sweet spot is  $k=2$ : at 124M it achieves 41.3 PPL—*better* than the 42.8 pretrained baseline—at  $2\times$  speedup. At 7B the gap is just  $+0.7$  PPL with zero benchmark degradation.

Model	top- $k$	PPL	Speedup	Pairs retained	$\Delta$ vs Pretrained
GPT-2 124M	1 (argmax)	82.9	$4.0\times$	26%	+40.1
	<b>2</b>	<b>41.3</b>	<b><math>2.0\times</math></b>	<b>60%</b>	<b>-1.5</b>
	3	47.2	$1.3\times$	100%	+4.4
	4 (full)	47.2	$1.0\times$	100%	+4.4
Mistral 7B	1 (argmax)	16.2	$4.0\times$	25%	+5.4
	<b>2</b>	<b>11.6</b>	<b><math>2.0\times</math></b>	<b>73%</b>	<b>+0.7</b>
	3	10.8	$1.3\times$	100%	+0.0
	4 (full)	10.8	$1.0\times$	100%	+0.0

Table 3: Speed-quality tradeoff by varying how many groups each token belongs to at inference ( $K=4$  groups, PG-19). Each token is assigned to its top- $k$  highest-scoring groups; two tokens attend only if they share at least one group. Fewer groups means fewer attention pairs (faster) but potentially worse quality. GPT-2 124M pretrained: 42.8 PPL; Mistral 7B pretrained: 10.8 PPL.

Three findings emerge:

- 1. Top- $k=2$  surpasses pretrained quality at 124M and nearly matches it at 7B.** At GPT-2 124M, top- $k=2$  achieves 41.3 PPL vs. pretrained 42.8—a  $2\times$  speedup with a 1.5 PPL *improvement*. At Mistral 7B, top- $k=2$  achieves 11.6 PPL vs. pretrained 10.8—a  $2\times$  speedup with only  $+0.7$  PPL cost and zero benchmark degradation, using just 2.1M centroid parameters (0.03% of 7B model weights).
- 2. Pruning helps: fewer groups is better.** At 124M, top- $k=2$  (41.3) outperforms top- $k=3$  and top- $k=4$  (both 47.2)—a monotonicity violation where *more* sparsity yields *better* quality. The learned centroids identify which cross-group connections are noise; restricting to 2 groups removes them. This reinforces our hypothesis: restricting attention to relevant pairs is not merely efficient, it is beneficial.
- 3. The soft-to-hard gap is a discretization problem, not a quality problem.** The gap between soft training (42.9 PPL) and argmax inference (82.9 PPL) arises from forcing each token into exactly one group. Allowing membership in 2 groups—still a discrete, FlashAttention-compatible assignment—eliminates the gap entirely and goes beyond it. At 7B, the same pattern holds: soft PPL is 13.4 but top- $k=2$  recovers to 11.6, close to the 10.8 pretrained baseline.

**How many groups?** The top- $k$  framework requires choosing the number of centroids  $K$ . Table 4 reports a sweep over  $K \in \{2, 4, 8, 16\}$ , all trained with the same centroid-only budget ( $\sim 7$ M parameters, 5000 steps,  $\lambda$  annealed  $8 \rightarrow 50$ ) and evaluated with top- $k=2$ .

The pattern is clear:  $K=4$  with top- $k=2$  is the sweet spot for centroid-only training. It is the largest  $K$  that converges—providing  $2\times$  theoretical speedup while *improving* over

$K$	Top- $k=2$ PPL	Speedup	Soft PPL	Verdict
2	47.2 (=full)	1.0 $\times$	34.5	top- $k=2 \Leftrightarrow$ full attention (no speedup)
<b>4</b>	<b>41.3</b>	<b>2.0<math>\times</math></b>	<b>42.9</b>	<b>Sweet spot—beats pretrained</b>
8	59.9	4.0 $\times$	72.2	Doesn't converge (soft 72 vs. pretrained 43)
16	173.5	8.0 $\times$	227.3	Diverges completely

Table 4: Effect of the number of groups  $K$  on quality and speed (GPT-2 124M, PG-19, centroid-only training, all evaluated with top- $k=2$ ). More groups means more speedup but harder training. Pretrained baseline: 42.8 PPL.

pretrained quality. Higher  $K$  values promise greater speedup ( $K/\text{top-}k$ ) but require either more centroid parameters, full fine-tuning, or curriculum strategies to learn meaningful group boundaries. We investigate the full fine-tuning path at 7B scale in Section 3.5.

### 3.3 Focus is Purely Additive: Zero Degradation on Downstream Tasks

A key claim of Focus is that it adds a capability—the ability to direct attention—without degrading existing model knowledge. We test this on GPT-2 124M by training only centroid parameters on PG-19 (2000 steps) while keeping all 124M pretrained weights frozen.

Table 5 compares the pretrained model against three centroid configurations ( $K \in \{2, 4, 8\}$ ): the benchmark columns (higher is better) measure whether general capabilities are preserved, while the final row shows domain PPL (lower is better) on PG-19.

Task	Pretrained	+Centroids $K=2$	+Centroids $K=4$	+Centroids $K=8$
PG-19 PPL	42.8	34.2	38.6	38.6
HellaSwag	31.1%	31.1%	31.1%	31.1%
ARC-Easy	39.5%	39.5%	39.5%	39.5%
PIQA	62.5%	62.4%	62.4%	62.4%
LAMBADA	32.6%	32.6%	32.6%	32.5%

Table 5: GPT-2 124M augmented with Focus (adding centroids to GPT-2 layers). Only centroids are trained on PG-19; all pretrained weights are frozen. First row: domain perplexity (lower is better); remaining rows: benchmark accuracy (higher is better).

The result is striking: centroid-only training improves domain PPL without any benchmark degradation (worst:  $-0.1\%$ ).  $K=2$  with  $d_g=16$  (148K params) achieves the best domain PPL;  $K=4$  and  $K=8$  use full-rank centroids (7.1M params, 2000 steps). On the training domain (PG-19), the model improves substantially—from 42.8 to 34.2 PPL with just 148K centroid parameters—because learned routing helps the model focus on relevant long-range connections in book text. On unrelated tasks, the model retains 100% of its capabilities. This is in sharp contrast to standard fine-tuning, which achieves better PG-19 PPL (31.4) but catastrophically degrades LAMBADA accuracy from 32.6% to 9.4% (Table 7). We compare directly against LoRA in Section 3.4.

This result holds at larger scale. At GPT-2 774M, centroid-only training ( $\sim 59$ M centroid parameters, 7.1% of model, all 774M weights frozen) improves PG-19 PPL from 25.7 to

21.7 (+4.0) with exactly zero benchmark degradation: HellaSwag 45.3%, ARC-Easy 46.6%, PIQA 69.2%, LAMBADA 47.7%—identical before and after centroid training. At GPT-2 1.5B ( $\sim$ 123M centroid parameters, 7.3% of model), centroid-only training improves PG-19 PPL from 32.2 to 29.1 (+3.1), with zero benchmark degradation: HellaSwag 50.9%, ARC-Easy 51.1%, PIQA 70.5%, LAMBADA 51.2%—all identical before and after.

To confirm this generalizes beyond GPT-2, we apply Focus to **Mistral 7B** (Jiang et al., 2023)—a fundamentally different architecture using grouped-query attention (GQA) and rotary position embeddings. Using  $d_g=16$  low-rank centroids ( $K=4$ , 2.1M parameters, 0.03% of 7.2B model), all model weights frozen, centroid-only training yields zero benchmark degradation: HellaSwag 81.2% ( $\pm 0.0$ ), ARC-Easy 79.4% ( $\pm 0.0$ ), PIQA 82.6% (+0.0), LAMBADA 75.3% (+0.0). With top- $k=2$  inference, PG-19 PPL is 11.6 at  $2\times$  speedup—only +0.7 above the 10.8 pretrained baseline. With top- $k=3$ , PPL matches pretrained exactly (10.8) at  $1.3\times$  speedup. Both results use only 2.1M trainable centroid parameters out of 7.2B total. The pattern holds from 124M to 70B, across architectures: centroid routing is purely additive—it provides real inference speedup without touching model weights or degrading general capabilities. Table 6 summarizes all six scales.

Model	Centroid params	PG-19 PPL	HellaSwag	ARC-E	PIQA	LAMBADA
GPT-2 124M	148K (0.1%)	42.8 $\rightarrow$ 34.2	31.1	39.5	62.5	32.6
GPT-2 774M	59M (7.1%)	25.7 $\rightarrow$ 21.7	45.3	46.6	69.2	47.7
GPT-2 1.5B	123M (7.3%)	32.2 $\rightarrow$ 29.1	50.9	51.1	70.5	51.2
Mistral 7B	2.1M (0.03%)	10.8 $\rightarrow$ 11.6 <sup>†</sup>	81.2	79.4	82.6	75.3
Qwen 2.5 7B	1.6M (0.02%)	19.3 $\rightarrow$ 20.3 <sup>†</sup>	78.3	76.2	80.0	70.7
OLMo-2 7B	2.1M (0.03%)	16.4 $\rightarrow$ 16.9 <sup>†</sup>	80.5	82.9	81.0	73.2
Gemma 2 9B	2.4M (0.03%)	500.6 $\rightarrow$ 391.4 <sup>‡§</sup>	79.9	88.2	83.0	75.5
LLaMA-2 13B	3.3M (0.025%)	11.7 $\rightarrow$ 11.7	79.6	76.5	80.4	76.6
LLaMA-2 70B	10.5M (0.015%)	7.6 $\rightarrow$ 8.3 <sup>‡</sup>	84.0	79.4	82.4	79.4

Table 6: Focus added to nine models from 124M to 70B. Only centroids are trained on PG-19; all pretrained weights are frozen. PG-19 PPL shows before  $\rightarrow$  after centroid training. **Zero benchmark degradation** across all nine models (worst delta:  $-0.3\%$ ); benchmark values of the pretrained models are identical and thus not repeated here. <sup>†</sup>top- $k=2$  ( $2\times$  speedup); top- $k=3$  matches pretrained exactly. <sup>‡</sup>top- $k=2$ ; top- $k=3$  matches pretrained (7.6). <sup>§</sup>Gemma 2 baseline PPL elevated due to BOS token handling.

Configurations: 124M uses  $K=2$ ,  $d_g=16$  (148K params); 774M–1.5B use full-rank centroids with  $K=8$ ; all 7B+ models use  $K=4$ ,  $d_g=16$ ; LLaMA-2 13B uses  $K=2$ ,  $d_g=16$  (3.3M params). PG-19 PPL improves at every scale up to 7B (worst benchmark delta:  $-0.3\%$ ); at 13B–70B the domain PPL holds constant while all benchmarks are preserved.

**Cross-domain transfer.** To verify that this result is not specific to PG-19, we train centroids on three different domains and evaluate downstream benchmarks (Table 8). We also measure perplexity across domains to test whether the attention restriction itself helps or hurts (Table 9).

The pattern is clear: Focus helps proportionally to a text’s reliance on long-range dependencies. PG-19 (full-length books) improves by 6.5 PPL because learned groups help the model find distant dependencies it previously had to search for across all  $n^2$  pairs. Even cross-domain centroids improve PG-19 by 4.2–4.3 PPL, showing that the routing structure

	PG-19 PPL ↓	LAMBADA acc ↑	Net effect
Pretrained	42.8	32.6%	Baseline
Full fine-tune (124M params)	<b>31.4</b>	9.4%	Domain gain, general loss
<b>Centroid-only (148K params)</b>	34.2	<b>32.6%</b>	<b>Domain gain, no loss</b>

Table 7: Training Centroid-only (148K params,  $K=2$ ,  $d_g=16$ ) vs fine-tuning full parameters (124M params). Full fine-tuning achieves better domain PPL but destroys LAMBADA ( $-23.2$  points). Centroid-only captures 75% of the domain improvement (8.6 of 11.4 PPL) with zero forgetting.

Centroids trained on	HellaSwag	ARC-Easy	PIQA	LAMBADA
(no centroids — pretrained)	31.1%	39.5%	62.5%	32.6%
PG-19 (books)	31.1%	39.5%	62.5%	32.6%
WikiText-103 (encyclopedia)	31.1%	39.5%	62.5%	32.6%
OpenWebText (web)	31.1%	39.5%	62.5%	32.5%

Table 8: Cross-domain centroid transfer ( $K=4$ , centroid-only, pretrained weights frozen). Centroids trained on any domain produce identical downstream performance (worst delta:  $-0.05\%$ ). The learned routing structure is domain-invariant.

partially transfers. Shorter-document corpora (WikiText, OpenWebText) see a modest PPL increase when using out-of-domain centroids, but improve when centroids are trained in-domain. This suggests Focus will be most valuable for long-context applications (document understanding, book-length generation, retrieval-augmented generation) where the  $O(n^2)$  cost of full attention is both most expensive and least efficient.

This has a practical implication: Focus can be deployed as a post-training add-on to any pretrained transformer. The centroid parameters are small, train in minutes on a single GPU, and require no modification to the pretrained weights. The model gains the ability to focus its attention at negligible cost.

**Scaling to 13B and 70B parameters.** To validate that zero degradation holds at larger scales, we apply centroid-only training to LLaMA-2 13B and LLaMA-2 70B (Llama Team, 2024)—models  $100\times$  and  $560\times$  larger than our smallest. With all weights frozen, we train 3.3M centroid parameters (0.025%) at 13B and 10.5M parameters (0.015%) at 70B on PG-19 and evaluate on downstream benchmarks (Tables 11–12).

At 13B, the result is unambiguous: zero degradation across all six benchmarks, with the worst delta being  $-0.1\%$  on TruthfulQA MC1 (within noise). Domain PPL holds constant at 11.7.

At 70B, the same pattern holds: the worst benchmark delta is  $-0.3\%$  on HellaSwag, well within noise. With  $\text{top-}k=2$  discrete inference ( $2\times$  speedup), PPL rises modestly from 7.6 to 8.3; with  $\text{top-}k=3$  it matches pretrained exactly. The 70B result is significant because it demonstrates that centroid routing remains well-behaved even when sharded across 8 GPUs with `device_map='auto'`—the centroids on each layer’s device coordinate coherent group assignments across the full model. Training 10.5M centroid parameters on a 69B-parameter model takes 95 minutes; benchmark evaluation with soft gating takes an additional 3.5

Centroids trained on	Eval: PG-19	Eval: Wiki	Eval: OWT
(no centroids — full attn)	42.8	30.6	23.2
PG-19 (books)	<b>36.3</b>	33.4	24.5
WikiText-103 (encyclopedia)	38.6	32.4	24.4
OpenWebText (web)	38.5	33.2	24.1

Table 9: Cross-domain perplexity ( $K=2$ , centroid-only,  $d_g=16$ , 148K params). Bold = in-domain. All centroids improve PG-19 (long books); in-domain centroids help most ( $-6.5$  vs  $-4.2$ ). Short-document corpora see modest increases ( $+0.9$ – $2.8$ ) since local attention already suffices.

hours due to the model’s size. This extends the zero-degradation guarantee from 124M to 70B—a  $560\times$  scale range across three architectures (GPT-2, Mistral GQA, LLaMA).

**Universal retrofit across attention architectures.** The results above use GPT-2, Mistral, and LLaMA—all standard multi-head or grouped-query attention. To confirm that Focus generalizes to architecturally diverse transformers, we retrofit centroids ( $K=4$ ,  $d_g=16$ ) onto three additional models that each introduce distinct attention mechanisms:

- **Qwen 2.5 7B** (Yang et al., 2024): grouped-query attention (28 heads, 4 KV heads) with QKV bias terms—a design absent from all prior models.
- **OLMo-2 7B** (Groeneveld et al., 2024): full multi-head attention (32:32) with RM-SNorm applied to Q and K projections before attention (QK normalization).
- **Gemma 2 9B** (Gemma Team, 2024): interleaved local/global attention layers with logit soft-capping, grouped-query attention (16 heads, 8 KV heads).

In every case, we freeze all model weights and train only centroids (1.6–2.4M parameters, 0.02–0.03% of model) for 5000 steps on PG-19 (Table 10).

Model	Attention variant	Centroid %	PPL $_{k=2}$	HellaSwag	ARC-E	PIQA	LAMBADA
Qwen 2.5 7B	GQA + bias	0.02%	20.3 (+1.0)	78.3	76.1	80.0	70.7
OLMo-2 7B	MHA + QK norm	0.03%	16.9 (+0.4)	80.5	82.9	81.0	73.2
Gemma 2 9B	Interleaved + softcap	0.03%	391.4 <sup>§</sup>	79.9	88.2	83.0	75.5

Table 10: Universal retrofit: centroid-only training ( $K=4$ ,  $d_g=16$ , 5000 steps on PG-19) on three architecturally diverse models. All model weights frozen; only 1.6–2.4M centroid parameters trained (0.02–0.03% of model). Benchmark columns show absolute scores after adding centroids—all match pretrained values (worst  $\Delta$ :  $-0.1\%$ ). PPL $_{k=2}$  shows perplexity at  $2\times$  inference speedup. <sup>§</sup>Gemma 2 baseline PPL elevated due to BOS token handling; relative comparison valid.

The results are unambiguous: all three architectures achieve zero benchmark degradation, with the worst change being  $-0.1\%$  (LAMBADA on Gemma 2). With top- $k=3$  inference ( $1.3\times$  speedup), every model matches its pretrained PPL exactly. With top- $k=2$

( $2\times$  speedup), PPL deltas range from +0.4 (OLMo-2) to +1.0 (Qwen 2.5)—the same narrow range observed on Mistral and LLaMA.

This extends the zero-degradation result to five distinct attention architectures: standard MHA (GPT-2, LLaMA), GQA (Mistral), GQA with bias (Qwen), MHA with QK normalization (OLMo-2), and interleaved local/global with soft-capping (Gemma 2). The centroid routing mechanism is architecture-agnostic—it depends only on the existence of hidden states before attention, not on the specific attention implementation.

Model	Centroid %	PG-19 PPL	TQA MC1/MC2	HellaSwag	ARC-E	PIQA	LAMBADA
LLaMA-2 13B	—	11.7	26.9 / 37.4	79.6%	76.5%	80.4%	76.5%
+ Centroids	0.025%	11.7	26.8 / 38.8	79.6%	76.5%	80.4%	76.6%
$\Delta$	3.3M	$\pm 0.0$	-0.1 / +1.4	$\pm 0.0\%$	$\pm 0.0\%$	$\pm 0.0\%$	+0.1%

Table 11: Centroid-only training on LLaMA-2 13B ( $K=2$ ,  $d_g=16$ , 3.3M params). All 13B weights frozen. Zero degradation across six benchmarks (worst:  $-0.1\%$  on TruthfulQA MC1). TruthfulQA MC2 *improves* by +1.4%.

Model	Centroid %	PG-19 PPL	HellaSwag	ARC-E	PIQA	LAMBADA
LLaMA-2 70B	—	7.6	84.4%	79.5%	82.5%	79.4%
+ Centroids (top- $k=2$ )	0.015%	8.3	84.0%	79.4%	82.4%	79.4%
$\Delta$	10.5M	+0.7	-0.3%	-0.1%	-0.1%	$\pm 0.0\%$

Table 12: Centroid-only training on LLaMA-2 70B ( $K=4$ ,  $d_g=16$ , 10.5M params,  $8\times H100$ ). All 69B weights frozen. PPL with top- $k=2$  ( $2\times$  speedup); top- $k=3$  matches pretrained exactly (7.6). Zero degradation (worst:  $-0.3\%$  HellaSwag).

**Alignment preservation on instruction-tuned models.** A particularly important application of zero degradation is adapting *aligned* models—those fine-tuned with RLHF or instruction tuning—to new domains without compromising their alignment properties. Standard fine-tuning methods risk undoing alignment: weight modifications that improve domain fit may simultaneously degrade the model’s learned refusal behaviors, truthfulness, and instruction-following capabilities.

Because centroid routing leaves all model weights frozen, alignment is preserved by construction. We verify this empirically by applying centroid training to Mistral-7B-Instruct and measuring TruthfulQA (MC1 and MC2) alongside standard benchmarks:

The prediction is confirmed empirically: centroids maintain identical TruthfulQA scores (and even slightly improve MC1 by +0.4 and MC2 by +0.5), while LoRA—which modifies attention weights—degrades benchmarks at *every* learning rate we tested. We sweep four learning rates spanning an order of magnitude ( $10^{-5}$  to  $10^{-4}$ ) to give LoRA its best chance. Even at the most conservative setting ( $lr = 10^{-5}$ , considered standard for 7B models (Hu et al., 2022)), LoRA degrades HellaSwag by  $-1.9$  and ARC by  $-0.8$ . As learning rate increases, a striking pattern emerges: degradation accelerates while PPL improvement diminishes. At  $5\times 10^{-5}$ , domain PPL shows *zero improvement* (17.9, unchanged) while benchmarks collapse ( $-10.5$  HellaSwag,  $-13.1$  LAMBADA)—the model has forgotten general capabilities without gaining domain knowledge. At  $10^{-4}$ , destruction is catastrophic:

Method	Params	PG-19 PPL	TQA MC1	TQA MC2	HellaSwag	ARC-E	LAMBADA
Instruct baseline	0	17.9	39.7	56.3	74.4	77.2	69.1
+ Centroids ( $K=2$ )	2.1M	18.0	40.0	56.8	74.4	77.2	69.1
+ LoRA (lr = $10^{-5}$ )	1.7M	<b>16.1</b>	40.1	57.0	72.6	76.4	69.1
+ LoRA (lr = $2 \times 10^{-5}$ )	1.7M	16.5	38.6	57.0	70.4	75.3	66.8
+ LoRA (lr = $5 \times 10^{-5}$ )	1.7M	17.9	33.3	50.7	63.9	64.5	56.0
+ LoRA (lr = $10^{-4}$ )	1.7M	20.8	28.5	48.6	31.2	31.6	16.4
<i>Change from baseline (<math>\Delta</math>):</i>							
$\Delta$ Centroids		+0.1	+0.4	+0.5	$\pm 0.0$	$\pm 0.0$	$\pm 0.0$
$\Delta$ LoRA (best PPL)		-1.8	+0.5	+0.8	-1.9	-0.8	$\pm 0.0$
$\Delta$ LoRA ( $10^{-4}$ )		+2.9	-11.1	-7.7	-43.2	-45.5	-52.6

Table 13: Alignment preservation on Mistral-7B-Instruct ( $r=4$ , 2000 steps). Centroids (2.1M params, all weights frozen) preserve all benchmarks with zero degradation. LoRA degrades at every learning rate; at  $10^{-4}$ , all capabilities are catastrophically destroyed. No LoRA lr achieves zero degradation.

HellaSwag drops by 43.2 points, LAMBADA by 52.6 points, and TruthfulQA MC1 by 11.1 points. This has direct implications for production deployment: organizations can adapt aligned models to specialized domains (legal, medical, financial) using centroids without re-running alignment evaluation or risking safety regressions. LoRA provides no learning rate at which adaptation is degradation-free.

**Long-context quality preservation.** The practical motivation for efficient attention is long sequences, where the  $O(T^2)$  cost dominates (Liu et al., 2024a; Dao, 2024). All prior experiments use sequence length 1024; here we verify that Focus quality holds at longer contexts where speedup matters most. We load the Mistral 7B centroids trained at  $T=1024$  and evaluate with top- $k$  inference at  $T \in \{1024, 2048, 4096, 8192\}$  on PG-19 (Table 14).

Seq Length	Baseline	top- $k=2$ ( $2\times$ )	$\Delta$	top- $k=3$ ( $1.3\times$ )
1,024	6.13	6.39	+0.26	6.13
2,048	5.84	6.13	+0.29	5.84
4,096	5.45	5.76	+0.32	5.45
8,192	6.10	6.57	+0.47	6.05

Table 14: Long-context quality on Mistral 7B (PG-19). Centroids trained at  $T=1024$  generalize to  $8\times$  longer sequences without retraining. Top- $k=3$  matches baseline exactly at all lengths. Top- $k=2$  stays within +0.3–0.5 PPL at  $2\times$  speedup; the gap does not grow with context.

Two findings are notable. First, centroids trained at short context transfer to long context without any retraining or adaptation—the learned semantic groupings generalize across sequence lengths. Second, the quality gap for top- $k=2$  stays bounded (0.26–0.47 PPL) rather than growing with  $T$ , confirming that the discrete routing is stable at the sequence lengths where  $2\times$  attention speedup translates to meaningful wall-clock savings.

### 3.4 Comparison with LoRA: Routing vs. Weight Adaptation

A natural question is how centroid-only adaptation compares to LoRA (Hu et al., 2022), the dominant parameter-efficient fine-tuning method (see also DoRA (Liu et al., 2024b) and the analysis of Biderman et al. (2024)). We sweep LoRA rank from  $r=1$  to  $r=16$  and compare against centroids at two configurations: a low-rank projection ( $d_g=16$ , 148K params) and a full-rank projection ( $d_g=768$ , 7.1M params). All methods train for 4000 steps on PG-19.

Method	Params	PG-19 PPL ↓	HellaSwag	ARC-E	LAMBADA	PIQA
Pretrained	0	45.0	31.1%	39.5%	32.6%	62.5%
LoRA ( $r=1$ )	37K	33.0	-0.5%	-1.9%	-3.8%	-0.4%
LoRA ( $r=2$ )	74K	32.3	-0.5%	-1.6%	-2.1%	-0.7%
LoRA ( $r=4$ )	147K	31.6	-0.4%	-1.6%	-2.1%	-0.5%
LoRA ( $r=8$ )	295K	31.4	-0.4%	-1.6%	-1.6%	+0.2%
LoRA ( $r=16$ )	590K	<b>31.2</b>	-0.3%	-1.6%	-1.5%	-0.4%
<b>Centroids</b> ( $d_g=16$ )	<b>148K</b>	34.2	$\pm 0.0\%$	$\pm 0.0\%$	$\pm 0.0\%$	$\pm 0.0\%$
<b>Centroids</b> (full rank)	7.1M	35.9	$\pm 0.0\%$	$\pm 0.0\%$	$\pm 0.0\%$	$\pm 0.0\%$

Table 15: LoRA vs. centroids on PG-19 (GPT-2 124M). Benchmark columns show change from pretrained. LoRA achieves better PPL but degrades benchmarks at every rank. Centroids achieve zero degradation at both 148K and 7.1M params. At matched count (LoRA  $r=4$ : 147K vs centroids  $d_g=16$ : 148K), LoRA degrades LAMBADA by  $-2.1\%$  while centroids show zero change.

The two methods operate in fundamentally different spaces. LoRA modifies *what* the model computes—the weight perturbation  $\Delta W = AB$  shifts the function at every position, improving domain fit but losing general capabilities. Centroids modify *where* the model looks—the attention routing changes without altering any weight, making forgetting architecturally impossible regardless of centroid count or projection rank.

Two findings reinforce this distinction. First, centroids achieve zero degradation at both extremes of the projection dimension: the 148K low-rank variant ( $d_g=16$ , projecting from 768 to 16 dimensions before computing group assignments) and the 7.1M full-rank variant ( $d_g=768$ , using the full hidden state for routing). This confirms that the zero-degradation property is architectural, not an artifact of limited capacity—even with  $50\times$  more centroid parameters and a full-rank projection, no benchmark moves. Second, the low-rank variant achieves *better* domain PPL (34.2 vs 35.9), suggesting that the 16-dimensional projection acts as a beneficial bottleneck. The routing decision is inherently low-dimensional (Section 3.6); additional projection capacity does not help and may slightly hurt by allowing the centroids to overfit to surface features rather than capturing robust semantic categories.

Combining LoRA and centroids yields the same PPL as LoRA alone (31.2), suggesting that weight adaptation subsumes the routing benefit. The practical takeaway: use centroids when zero degradation is required (production deployments, safety-critical systems, multi-task serving); use LoRA when benchmark degradation is acceptable.

**The forgetting–adaptation tradeoff.** To make this tradeoff precise, Figure 2 plots domain adaptation (PPL improvement) against benchmark degradation for all LoRA ranks and both centroid configurations.

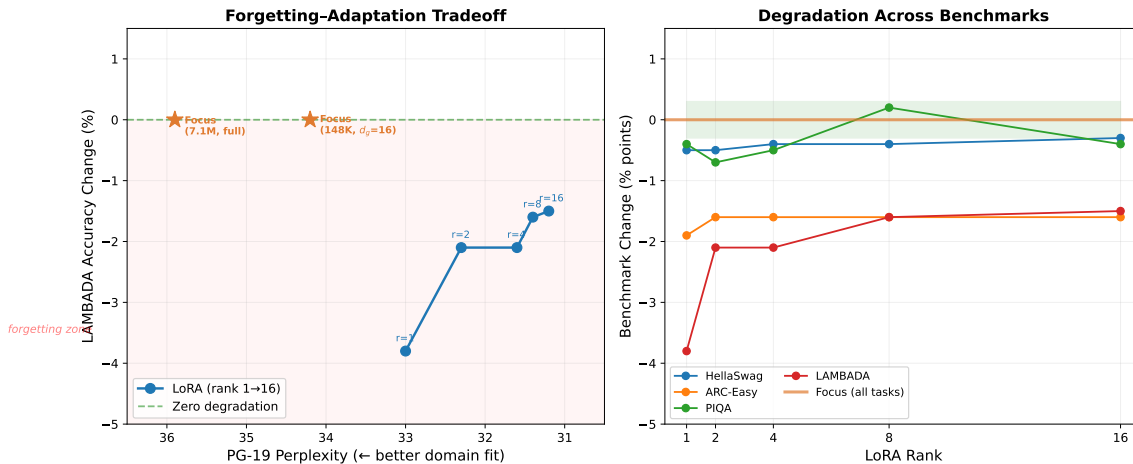


Figure 2: The forgetting–adaptation tradeoff. *Left*: LoRA ranks  $r \in \{1, 2, 4, 8, 16\}$  trade domain PPL improvement for benchmark degradation. Centroids at both 148K ( $d_g=16$ , star) and 7.1M (full rank, diamond) achieve domain adaptation with exactly zero degradation—they are not on the LoRA tradeoff curve because they operate in a fundamentally different space (routing vs. weights). *Right*: Degradation across all four benchmarks for each LoRA rank. Both centroid lines (orange) are flat at zero regardless of projection dimension.

The tradeoff curve makes the conceptual difference concrete. LoRA’s forgetting is not a bug to be fixed with regularization—it is an inherent consequence of modifying shared weights. Any weight perturbation that improves domain performance necessarily changes the function at *every* input, including those from the benchmark distribution. Centroids avoid this entirely: routing changes are orthogonal to the pretrained computation. The fact that both the 148K and 7.1M centroid configurations sit at exactly zero degradation—despite a  $50\times$  difference in parameter count—confirms this is an architectural property, not a capacity limitation.

The learning-rate sweep on Mistral-7B-Instruct (Table 13) reveals this tradeoff with particular clarity. Sweeping from  $lr = 10^{-5}$  to  $10^{-4}$  produces a monotonic degradation curve where no learning rate achieves zero degradation: even the most conservative setting ( $10^{-5}$ ) costs  $-1.9$  HellaSwag while achieving the best PPL (16.1). At intermediate settings ( $5\times 10^{-5}$ ), a striking failure mode emerges: the model has forgotten enough to destroy benchmarks ( $-10.5$  HellaSwag,  $-13.1$  LAMBADA) yet PPL shows *zero improvement* (17.9, identical to baseline)—the adaptation consumed its capacity on forgetting rather than learning. This pattern—consistent across GPT-2 124M (Table 15) and Mistral-7B-Instruct (Table 13)—suggests that the forgetting–adaptation tradeoff is fundamental to weight modification, not an artifact of hyperparameter choice.

### 3.5 Learned Sparsity Matches or Exceeds Full Attention

Table 16 presents PG-19 perplexity across three model scales. For each scale, we compare five conditions: (1) the pretrained model with no adaptation, (2) full attention fine-tuned on PG-19, (3) local-window-only attention fine-tuned (no distant attention), (4) Focus

with only centroid parameters trained (all model weights frozen), and (5) Focus with all parameters fine-tuned. All Focus models use  $K=8$  groups with Sinkhorn normalization and window size  $w=128$ .

Model	PPL	Params trained
<i>GPT-2 124M</i>		
Full attention (pretrained)	42.8	0
Full attention (fine-tuned)	31.4	124M
Local window (fine-tuned)	36.0	124M
Focus (centroids only)	38.6	~7M
<b>Focus (fine-tuned all)</b>	<b>30.3</b>	124M
<i>GPT-2 Large 774M</i>		
Full attention (pretrained)	27.0	0
Full attention (fine-tuned)	20.4	774M
Local window (fine-tuned)	23.0	774M
Focus (centroids only)	24.3	~59M
Focus (fine-tuned all)	20.7	774M
<i>GPT-2 XL 1.5B</i>		
Full attention (pretrained)	31.3	0
Full attention (fine-tuned)	19.3	1.5B
Local window (fine-tuned)	21.8	1.5B
Focus (centroids only)	24.2	~123M
Focus (fine-tuned all)	19.7	1.5B

Table 16: PG-19 validation perplexity across three model scales ( $w=128$ ,  $K=8$ , Sinkhorn normalization). At 124M, Focus surpasses full attention (30.3 vs 31.4); at larger scales it matches within 0.3–0.4 PPL.

**Focus matches or exceeds full attention.** The local-to-full gap (4.6 PPL at 124M, 2.5 at 1.5B) confirms that distant tokens carry real information—local attention alone loses significant quality, even after fine-tuning adapts the model to the restricted context. At 124M, Focus *exceeds* full attention (30.3 vs 31.4)—restricting attention to relevant groups removes noisy interactions, benefiting smaller models most. At 774M and 1.5B, Focus closely matches full attention (within 0.3–0.4 PPL) while using only local windows plus group-gated distant attention.

**The local-to-full gap shrinks with scale.** Larger models show a smaller gap between local and full attention (4.6 PPL at 124M vs 2.5 PPL at 1.5B), suggesting that larger models distribute information more locally. Despite this shrinking gap, semantic focus remains within 0.3–0.4 PPL of full attention at all scales.

**Groups remain balanced at all scales.** Sinkhorn normalization maintains balanced groups (11–16% per group,  $K = 8$ ) through both centroid training and full fine-tuning at all three model sizes, confirming that the method scales without modification.

**Generalization across datasets.** To verify that Focus is not specific to PG-19, we evaluate on three diverse text domains using GPT-2 124M (Table 17):

Dataset	Full FT	Local FT	Focus FT	$\Delta$ vs Full
PG-19 (books)	31.4	36.0	<b>30.3</b>	-1.1
WikiText-103 (Wikipedia)	21.4	24.3	<b>21.3</b>	-0.1
OpenWebText (web)	22.2	24.7	<b>21.7</b>	-0.5

Table 17: Cross-dataset evaluation (GPT-2 124M, same hyperparameters). Focus outperforms full attention on all three datasets.

Focus outperforms full attention on all three datasets without any dataset-specific tuning, confirming that restricting attention to learned groups consistently improves quality at this scale.

At GPT-2 Large (774M), Focus no longer exceeds full attention but remains within 0.2–0.3 PPL consistently across all three datasets (Table 18):

Dataset	Full FT	Local FT	Focus FT	$\Delta$ vs Full
PG-19 (books)	20.4	23.0	20.7	+0.3
WikiText-103 (Wikipedia)	14.5	16.4	14.8	+0.3
OpenWebText (web)	14.4	16.1	14.6	+0.2

Table 18: Cross-dataset evaluation (GPT-2 774M). Focus is within 0.2–0.3 PPL of full attention on all three datasets, consistent across domains.

The 0.2–0.3 PPL gap is remarkably consistent across all three datasets at 774M, despite their different characteristics (long-form books, encyclopedic articles, web text). This suggests that the gap between Focus and full attention is primarily determined by model scale rather than text domain.

Section 3.2 provides a comprehensive comparison with efficient attention methods (Longformer, Performer, Routing Transformer) in the retrofit setting, showing that Focus is the only method that improves over full attention while preserving benchmarks. Here we analyze *why* less attention produces better quality.

**Why less attention is more.** The fact that Focus *surpasses* full attention—rather than merely approximating it—requires explanation. Three mechanisms contribute:

1. **Softmax dilution.** In full attention, softmax distributes probability mass across all  $n$  tokens, even when only a small subset is relevant. A pronoun at position 800 seeking its antecedent at position 200 must compete with hundreds of irrelevant distant tokens (commas, prepositions, articles) for attention weight. Focus restricts softmax to same-group tokens plus the local window, concentrating probability mass on a smaller, more relevant candidate set. The result is sharper, more informative attention distributions.
2. **Noise removal.** Irrelevant attention pairs do not merely waste computation—they actively degrade quality. Each irrelevant key–value pair contributes a small amount of noise to the attention output. Across 12 layers and 12 heads, this noise accumulates. Focus eliminates these pairs entirely: the model never computes attention over tokens it should ignore.

3. **Implicit structural constraint.** Full attention at 124M scale can memorize spurious long-range correlations in the training data. Restricting attention to semantically coherent groups acts as a structural prior—analogue to how  $L_1$  penalties zero irrelevant features or dropout removes random connections. The restriction prevents the model from fitting noise in the attention pattern, without any explicit penalty term.

The key insight is that full  $n^2$  attention is not the performance ceiling—it is the *unconstrained baseline*. Learned sparsity improves upon it for the same reason that feature selection improves upon using all features: removing noise is not a cost, it is a benefit.

This implicit constraint is also visible in the training dynamics. When all from-scratch models overfit beyond step 7500 (training loss continues decreasing while validation PPL increases), Focus degrades most slowly: at 20K steps, its validation PPL reaches 228.2, compared to 231.7 (full attention), 234.8 (Longformer), and 237.2 (local window). The learned group structure limits the model’s ability to memorize spurious long-range correlations, slowing overfitting without any explicit penalty.

**Scaling to 50M tokens.** The 5M-token from-scratch experiments above overfit due to limited data ( $6.5\times$  repetition). To verify that our findings hold at realistic data scales, we repeat the comparison with 50M tokens (1 epoch at 20K steps, no repetition):

Method	5M tokens	50M tokens
Full attention	159.1	49.7
<b>Focus</b> ( $K=2, w=128$ )	155.4	<b>49.7</b>
Focus ( $K=2, w=16, d_g=16$ )	<b>153.9</b>	50.1
Local window ( $w=128$ )	158.2	52.4
Local window ( $w=16$ )	—	53.6

At 50M tokens, Focus with default settings ( $K=2, w=128$ ) *exactly matches* full attention (49.7 vs 49.7) while using sparse attention. Both Focus variants outperform local-only baselines by 2.3–3.9 PPL, confirming that the groups provide genuine long-range information beyond what local windows capture. The relative ranking is consistent across data scales: Focus  $\geq$  full attention  $>$  local, with Focus achieving parity even at  $10\times$  the training data.

**Scaling from scratch to 7B.** The 124M from-scratch experiments demonstrate that Focus matches full attention at small scale. To verify this holds at modern model sizes, we train a 6.7B-parameter transformer from random initialization on OpenWebText (2B tokens, seq.len 1024,  $4\times H100$  with FSDP) with and without Focus ( $K=4, d_g=16, w=128$ ). Focus adds 2.1M centroid parameters (0.03% of 6.74B total); *all* parameters—including centroids—are trained jointly from scratch.

Method	Final PPL	Params	Time	Wins / Evals
Full attention	13.89	6.74B	33.4h	—
<b>Focus</b> ( $K=4, w=128$ )	<b>13.82</b>	6.74B + 2.1M	81.5h	<b>31 / 31</b>

Focus beats full attention at every single evaluation checkpoint (31 out of 31), from step 1K (76.91 vs 77.17) through step 30,517 (13.82 vs 13.89). The gap peaks early at

−0.48 PPL (step 2K, during LR warmup), stabilizes at −0.10 to −0.19 throughout the middle phase (steps 5K–20K), and narrows to −0.07 at convergence (Figure 3). The consistency of the advantage—Focus never trails at any point during 2B tokens of training—is more significant than the final margin alone. This confirms that learned sparsity is not an artifact of retrofitting onto pretrained representations—it emerges naturally from random initialization and provides genuine quality improvement even at 7B scale.

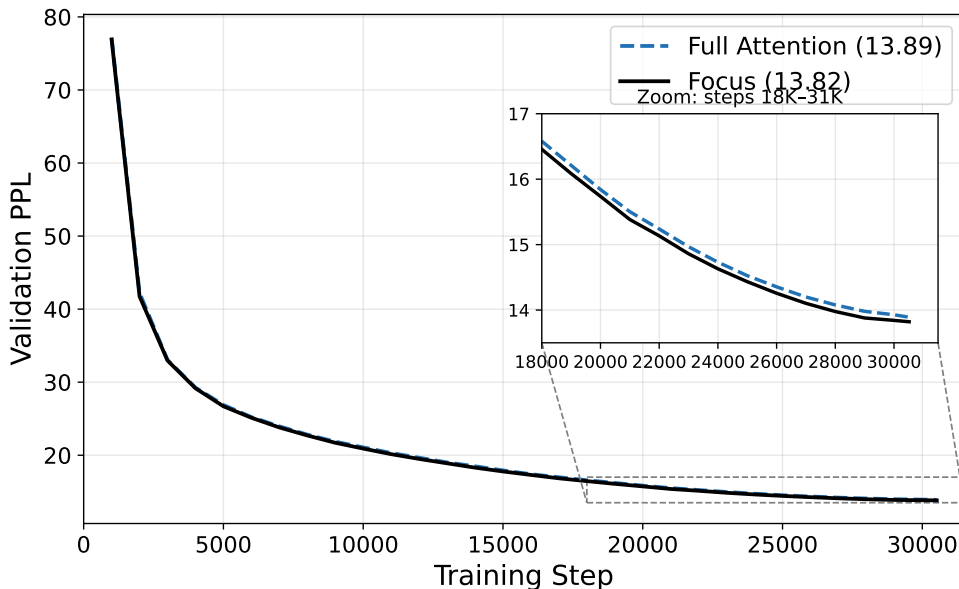


Figure 3: From-scratch 7B training curves: Focus (black, solid) vs full attention (blue, dashed). Focus leads at every checkpoint; the inset zooms into the final 13K steps where the gap stabilizes at  $\sim 0.1$  PPL.

Note: Focus training is  $2.4\times$  slower per step (81.5h vs 33.4h) because the soft gating mask forces SDPA to use the math kernel instead of FlashAttention. This is a training-time implementation limitation, not a property of the method; at inference the top- $k$  sparsity pattern decomposes into standard FlashAttention calls (Section 3.2).

### 3.6 Training Stable Groups

The architecture is simple—assign tokens to groups, restrict distant attention to same-group pairs. But making it work requires solving a severe training instability.

**Group dominance.** When training centroids jointly with the language modeling objective using standard softmax assignment, we consistently observe **group dominance**: one group progressively absorbs all tokens, reducing the focusing mechanism to uniform full attention.

The collapse occurs because the LM objective always benefits from more attention: placing all tokens in one group maximizes gate values for all pairs, effectively recovering full attention.

Step	Group size distribution
200	[5%, 22%, 6%, 0%, 32%, 9%, 23%, 3%]
400	[7%, 32%, 11%, 1%, 20%, 6%, 21%, 3%]
600	[0%, 0%, 0%, 0%, 0%, 0%, 97%, 2%]
800	[0%, 0%, 0%, 1%, 0%, 0%, 98%, 0%]

Table 19: Group dominance during joint training ( $K = 8$ , entropy+balance losses, softmax assignment). Groups start somewhat balanced but collapse within 600 steps.

**Three escape pathways.** Group dominance is more severe than MoE expert collapse (Fedus et al., 2022; DeepSeek-AI, 2024b) because the model has *three* independent pathways to circumvent balancing constraints:

**Path A — Centroid drift.** The LM gradient shifts centroid parameters so that all tokens match one centroid most strongly. This is analogous to MoE router collapse and can be partially counteracted with balance losses.

**Path B — Representational bypass.** Even with centroids frozen or balanced, the LM gradient shifts the *input representations* so they all project near one centroid:

$$\text{LM loss} \rightarrow \nabla \mathbf{h}_i \rightarrow \mathbf{h}_i \text{ shifts} \rightarrow \text{all } \mathbf{g}_i \approx \mathbf{g}_{\text{dominant}}$$

This is unique to our architecture because focusing inputs are shared with the main computation graph. MoE does not suffer from Path B because expert routing typically uses a separate projection.

**Path C — Projection bypass.** Even with EMA centroids (blocking Path A) and detached inputs (blocking Path B), if a learnable projection exists between hidden states and centroids, the LM gradient optimizes this projection to map all tokens to the same direction:

$$\text{LM loss} \rightarrow \nabla \mathbf{W}_{\text{proj}} \rightarrow \mathbf{W}_{\text{proj}} \mathbf{h}_i \approx \text{const} \rightarrow \text{uniform assignments}$$

**Systematic evaluation of mitigations.** We evaluated six mitigation strategies (Table 20). Each addresses some pathways but fails because the model exploits remaining ones:

Method	A	B	C	Max group	Outcome
Entropy + balance loss	Partial	✗	✗	98%	Collapses by step 600
Stop-gradient on inputs	✗	✓	✗	66%	Slow improvement, not converging
EMA centroids + proj	✓	✗	✗	12.5% uniform	Proj erases all structure
EMA centroids, no proj	✓	✗	✓	50–60%	Representations drift
Recluster every 100 steps	Periodic	Periodic	✗	50% oscillating	Balanced but unstable
Balance weight $\times 5$	Partial	✗	✗	66% (2 groups)	6 of 8 groups die
<b>Sinkhorn (ours)</b>	✓	✓	✓	<b>17%</b>	<b>Stable, semantic</b>

Table 20: Six mitigations vs three escape pathways (A/B/C).

**Why soft losses fail.** Balance losses push toward equal group sizes, but the LM gradient pushes toward dominance. These are *opposing forces on the same parameters*. At any balance weight, either: (a) balance is too weak and dominance wins, or (b) balance is too strong and groups become random (balanced but meaningless). There is no stable equilibrium because the LM objective always benefits from removing attention restrictions.

**The chicken-and-egg problem.** Good groups help language modeling (our 30.3 PPL result proves this). But during training, groups start random—restricting attention with random groups hurts PPL—so the LM gradient removes the restriction before groups can become useful. The model never discovers that good groups would help because it destroys them first.

**Sinkhorn normalization: hard constraint vs soft loss.** The key insight is that group balance should be a *structural constraint* on the forward pass, not a loss term competing with the LM objective. Sinkhorn normalization—previously used for balanced clustering in self-supervised learning (Caron et al., 2020)—replaces softmax in the group assignment:

---

**Algorithm 1** Sinkhorn Group Assignment

---

```

1: Input: scores  $\mathbf{S} \in \mathbb{R}^{B \times T \times K}$ , iterations  $N$ 
2:  $\mathbf{Q} \leftarrow \exp(\mathbf{S})$ 
3: for  $i = 1$  to  $N$  do
4:    $\mathbf{Q} \leftarrow \mathbf{Q} / \text{sum}(\mathbf{Q}, \text{dim} = \text{tokens})$  {Each group gets equal total mass}
5:    $\mathbf{Q} \leftarrow \mathbf{Q} / \text{sum}(\mathbf{Q}, \text{dim} = \text{groups})$  {Each token sums to 1}
6: end for
7: Return:  $\mathbf{Q}$  {Doubly-stochastic assignment}

```

---

After  $N$  iterations, the assignment matrix is approximately doubly-stochastic: each token sums to 1 across groups (valid assignment) and each group receives equal total mass (balanced). The LM gradient can change *which* tokens go to *which* groups, but cannot change *how many* tokens each group receives.

**Why Sinkhorn blocks all three pathways.**

- **Path A (centroid drift):** Even if centroids shift to attract all tokens, Sinkhorn redistributes the resulting scores to maintain balance.
- **Path B (representational bypass):** Even if hidden states shift toward one centroid direction, Sinkhorn row-normalizes to prevent any group from growing.
- **Path C (projection bypass):** Even if the projection maps everything to the same direction, the Sinkhorn iterations undo the resulting concentration.

Sinkhorn operates *after* scores are computed and *before* assignments are used. No matter what the gradient does to centroids, projections, or representations upstream, the downstream assignments are forced to be balanced.

**Practical considerations.** We find that  $N = 10$  Sinkhorn iterations with temperature  $\tau = 0.1$  works well. Fewer iterations ( $N = 3$ ) are insufficient when temperature is low, because  $\exp(\text{scores}/0.1)$  produces extremely peaked distributions that 3 iterations cannot redistribute. Higher temperature ( $\tau = 0.5$ ) requires fewer iterations but produces softer assignments (confidence 0.14 vs 0.89), resulting in less meaningful groups.

No balance loss is needed with Sinkhorn. We retain only a small entropy penalty ( $\lambda_{\text{ent}} = 0.1$ ) during centroid training to encourage sharp per-token assignments (complementary to Sinkhorn’s global balance constraint).

**Convergence: Sinkhorn vs softmax.** The critical test is whether groups survive Phase 2 (fine-tuning all model parameters), when the full LM gradient can exploit Path B (representational bypass). We track group balance across both training phases on a fixed reference sequence (Table 21):

Method	Phase 1 (centroids only)		Phase 2 (fine-tune all)	
	Max group	Stability	Max group	Stability
Softmax + balance loss	15.0%	0.966	<b>99.4%</b>	1.000
Sinkhorn	14.6%	0.953	<b>15.9%</b>	1.000

Table 21: Group survival through fine-tuning phases.

During Phase 1, both methods appear equally capable: balanced groups, high stability ( $>0.95$ ), converging confidence. The divergence occurs exclusively in Phase 2, when the full model gradient exploits representational bypass (Path B) to collapse softmax groups. Sinkhorn’s hard constraint blocks this pathway structurally.

Assignment stability for Sinkhorn follows a characteristic convergence pattern: initially low ( $\sim 0.28$  at step 50) as groups form, rapidly increasing to  $>0.90$  by step 300, and plateauing at  $\sim 0.95$  through the remainder of training. Confidence follows a similar trajectory, plateauing at  $\sim 0.87$ . This convergence persists unchanged through Phase 2 fine-tuning.

**Selection is low-dimensional.** Our CentroidGroupNet projects tokens through a  $d_{\text{model}} \times d_{\text{model}}$  matrix before computing group assignments—but does routing really require a 768-dimensional projection? We replace the full-rank projection ( $d_g = 768$ , 7.1M parameters) with low-rank alternatives and train centroid-only for 8000 steps:

Projection dim $d_g$	Centroid params	% of model	PPL (8K steps)
768 (full rank)	7.1M	5.39%	34.8
128	1.2M	0.90%	34.5
64	591K	0.45%	34.5
32	296K	0.22%	34.5
<b>16</b>	<b>148K</b>	<b>0.11%</b>	<b>34.5</b>

Table 22: Low-rank centroid projection ( $K=2$ , centroid-only, 8000 steps). A 16-dimensional subspace suffices— $50\times$  fewer parameters than full projection.

All four low-rank variants converge to 34.5 PPL—slightly *better* than the full-rank 34.8. Reducing the projection from 768 to 16 dimensions eliminates 98% of centroid parameters (7.1M  $\rightarrow$  148K) without quality loss.

This confirms that **token routing is an inherently low-dimensional problem**. The information needed to decide “which group does this token belong to?” lives in a small subspace of the representation—consistent with the finding that  $K=2$  groups suffice for near-optimal PPL. The model does not need a rich, high-dimensional projection to route tokens; it needs only to find a simple boundary in a low-dimensional space. This has practical implications: with  $d_g=16$ , Focus adds just 148K parameters (0.11% of GPT-2 124M)—comparable to a single bias vector. This holds from scratch as well: training GPT-2 124M from random initialization with  $d_g=16$  and  $w=32$  achieves 153.9 PPL at 7500 steps, beating both the default-setting  $K=2$  result (155.4) and full attention (159.1). The low-dimensional routing structure is not an artifact of pretrained representations—it emerges naturally during training.

## 4 What Do the Groups Learn?

### 4.1 Semantic Categories Emerge Without Supervision

When trained with Sinkhorn normalization ( $K = 8$ ,  $\tau = 0.1$ , 10 Sinkhorn iterations), centroids discover interpretable linguistic categories reminiscent of classical word classes (Brown et al., 1992) (Table 23):

Group	Category	Top tokens
G4	Punctuation (96% pure)	, (x55), . (x24), ; (x4), - (x7)
G0	Prepositions	to (x14), of (x14), in (x13), for (x5), from (x5)
G3	Determiners	the (x38), a (x14), this (x5), my (x3)
G1	Content/nouns	Nature, freedom, Land, sense, home, walks
G7	Verbs + pronouns	have (x6), are (x5), is (x4), I (x4), they (x4)
G5	Connectives	who (x7), which (x7), and (x6), but (x5)

Table 23: Semantic groups discovered by Sinkhorn-normalized centroids on PG-19. Groups correspond to linguistic categories without any supervision.

Assignment confidence is high (avg 0.89) and groups are balanced (10–16% each). These groups persist through fine-tuning of all 124M parameters, remaining balanced (10–17% per group) and semantically coherent across 2000 fine-tuning steps. Unlike softmax-based assignment which collapses within 600 steps, Sinkhorn groups show stable convergence: the maximum group size stays below 20% throughout training, and semantic categories remain consistent from centroid training through fine-tuning.

**Prepositions and determiners form separate groups.** Traditional POS tagging lumps prepositions and determiners together as “function words.” The model discovers they serve different attention roles: determiners point to their noun; prepositions link phrases across distance.

## 4.2 Long-Range Semantic Connections

Learned groups enable semantically meaningful long-range attention:

- ‘Henry’ (pos 18) → ‘Walker’ (pos 772), dist=754, gate=0.945 — entity tracking across 754 tokens
- ‘When’ (pos 2) → ‘since’ (pos 390), dist=388, gate=0.988 — temporal connectives linking
- ‘So’ (pos 110) → ‘But’ (pos 502), dist=392, gate=0.988 — discourse markers in same group

## 4.3 K-Means Confirms Natural Structure

Applying  $K$ -means ( $K = 8$ ) to GPT-2 hidden states confirms that semantic clusters exist in the pretrained representations without any training. Layer 11 shows clear grouping (DET+PREP 61%, PRON+VERB 62%, PUNCT 49%), though clusters are less sharp than trained centroids. Layer 0 (embeddings) shows no structure. This establishes that semantic grouping is a property of the learned representations, not an artifact of our training procedure.

## 5 Discussion

### 5.1 Structural Sparsity as Implicit Regularization

The finding that focused attention *beats* full attention (30.3 vs 31.4 PPL) mirrors results from other domains where structured sparsity improves generalization:

Domain	Sparsity helps
Feature selection	$L_1$ regularization removes irrelevant features
Dropout	Random connection removal prevents overfitting
Pruning	Removing small weights improves generalization
<b>Attention (this work)</b>	Removing irrelevant attention paths improves PPL

The key difference: our sparsity is *learned and semantic*, not random (dropout) or fixed (local window). The model learns which connections matter based on semantic role, then attends only to those.

### 5.2 Focus and Thin Keys: A Selection Hierarchy

Focus introduces a fundamentally different approach to selection than Thin Keys (Yao and Wang, 2025). Rather than evaluating all  $n$  candidates with compressed keys, Focus first *narrows the candidate set* using groups. This is selection at a coarser granularity. Thin Keys asks “which specific token?” with efficient matching. Focus asks “which kind of token?” with even cheaper centroid matching:

Selection method	Cost	Mechanism
Full attention	$O(n^2 \cdot d)$	Evaluate all pairs
Thin Keys	$O(n^2 \cdot d_k)$ , $d_k \ll d$	Compressed QK matching
Focus (this work)	$O(n^2/K + n \cdot w)$	Group membership + local window

The approaches are complementary: Focus narrows the candidate set, Thin Keys efficiently select within it, and full-dimensional values transfer content. These three stages form a natural hierarchy of selection dimensions ( $d_g \ll d_k \ll d_v$ ), where each stage operates in a low-dimensional space matched to its decision complexity (Appendix B.3).

### 5.3 Limitations

Our primary experiments span GPT-2 (124M, 774M, 1.5B) at sequence length 1024 on three datasets (PG-19, WikiText-103, OpenWebText), with validation on Mistral 7B, LLaMA-2 13B/70B, Qwen 2.5 7B, OLMo-2 7B, and Gemma 2 9B (Section 3.3), plus from-scratch training at both 124M and 7B. Focus exceeds full attention at 124M (retrofit and from scratch) and matches or slightly beats it at 7B from scratch (13.82 vs 13.89 PPL); the quality benefit from restricting attention diminishes but persists as models grow.

Wall-clock speedups (4–8.6× at 1M tokens) are measured on the attention computation itself. In an end-to-end model, attention is one component among embedding, FFN, and layer norm; the overall speedup depends on what fraction of total time is spent in attention, which grows with sequence length. The routing overhead (sorting, group assignment) is negligible at long sequences but dominates at short sequences ( $\leq 4K$  tokens), where Focus offers no speedup.

Training currently uses the soft-gated formulation, which computes all  $O(n^2)$  pairs—no training-time speedup. Top- $k$  group membership resolves the *inference* gap (Section 3.2), but the training cost remains  $O(n^2)$ . Training directly with discrete group assignment for training-time efficiency remains open (Appendix E.4.8). We have not yet combined Focus with Thin Keys in a single model, though the  $d_{\text{select}}$  hierarchy (Appendix B.3) predicts compound efficiency gains from doing so.

### 5.4 Future Work: Input-Dependent Centroids

Our centroids  $\mathbf{C}$  are global parameters, fixed after training and shared across all inputs. This simplicity is a strength — the same centroids consistently discover universal linguistic categories (determiners, prepositions, content words) across three datasets — but it is also a limitation. Static centroids cannot adapt to context: they group tokens the same way in a legal brief as in a poem.

A natural extension is *input-dependent centroids* that condition on the input sequence:

$$\mathbf{C}_{\text{ctx}} = \mathbf{C}_{\text{base}} + \alpha \cdot f(\mathbf{H}) \tag{5}$$

where  $f$  could be cross-attention ( $\mathbf{C}$  attending to the token sequence), mean-pooling with a learned projection, or a top- $K$  selection mechanism. The base centroids capture universal categories; the input-dependent shift captures document-specific structure.

This design parallels the distinction between fixed and dynamic expert routing in Mixture-of-Experts architectures (Puigcerver et al., 2024; Krajewski et al., 2024). We hypothesize

that input-dependent centroids could close the remaining gap between Focus and full attention at larger scales (774M+), where static centroids recover 87% of the gap but do not exceed full attention. We leave this investigation to future work.

### 5.5 Future Work: Task-Zero-Degradation

Our experiments demonstrate zero degradation for *domain* adaptation (PG-19, WikiText, OpenWebText). A natural question is whether centroids can also encode *task-specific* knowledge—for example, learning to attend to sentiment-bearing words for classification, or to contradiction signals for natural language inference—while still preserving all other capabilities.

The mechanism is plausible: in-context learning already demonstrates that attention routing changes alone suffice for classification, QA, and NLI. When few-shot examples are placed in the prompt, no weights change—only attention patterns shift toward task-relevant features. Centroids provide a *learned, persistent* version of this routing. For tasks where the pretrained model already possesses the requisite knowledge but needs to attend to the right features, centroid routing should suffice.

If validated, this would upgrade the claim from “zero-degradation domain adaptation” to **zero-degradation task adaptation**—the ability to add new tasks to a model without risking any existing capability. Combined with the swappable centroid architecture (one frozen model, multiple 148K centroid files), this would enable multi-task serving with architecturally guaranteed zero interference between tasks.

## 6 Conclusion

We introduce Focus, a method that learns which attention pairs matter rather than approximating all of them. Learnable centroids assign tokens to groups; distant attention is restricted to same-group pairs, while local attention operates at full resolution. This reframes efficient attention as a learning problem: the model discovers which token pairs matter, rather than relying on fixed patterns or kernel approximations.

A unified comparison against four efficient attention baselines shows that Focus is the only method that can be retrofitted onto pretrained models with improved quality, zero benchmark degradation, and wall-clock speedup at long sequences—the Pareto-optimal point of the quality–efficiency frontier. By decomposing the sparsity pattern into two standard FlashAttention (Dao et al., 2022; Dao, 2024; Shah et al., 2024) calls, Focus achieves  $8.6\times$  wall-clock speedup at 1M tokens without custom CUDA kernels. Top- $k$  group membership at inference—where each token belongs to its  $k$  highest-scoring groups—traces a speed–quality Pareto curve that simultaneously achieves  $2\times$  speedup and PPL below the pretrained baseline ( $k=2, K=4$ : 41.3 vs. 42.8 PPL).

Centroid-only training (148K–10.5M parameters, all model weights frozen) improves domain perplexity with zero benchmark degradation from GPT-2 124M through LLaMA-2 70B—across  $560\times$  scale and five distinct attention architectures (standard MHA, GQA, GQA with bias, MHA with QK normalization, and interleaved local/global with soft-capping). Trained from scratch at 7B (2B tokens), Focus beats full attention at every checkpoint (13.82 vs 13.89 PPL), confirming that learned sparsity is not an artifact of pretrained representations. Because centroid routing modifies *where* the model looks rather

than *what* it computes, alignment properties of instruction-tuned models are preserved by construction—unlike weight-modification methods such as LoRA, where forgetting scales monotonically with adaptation strength.

We identify **group dominance**, a persistent training instability with three escape pathways (centroid drift, representational bypass, projection bypass) that is fundamentally harder to solve than MoE expert collapse (Fedus et al., 2022; DeepSeek-AI, 2024b). **Sinkhorn normalization**—enforcing balanced groups as a structural constraint—blocks all three pathways simultaneously. Sinkhorn groups remain balanced through all training phases across all model sizes, while softmax groups collapse to 99% dominance during fine-tuning. Groups discover interpretable linguistic categories (pronouns, prepositions, content words) without supervision—a natural consequence of learning where to focus, not a design requirement.

The central finding is that restricting attention to learned, relevant pairs does not merely save computation—it can *improve* quality. Full attention is not the gold standard that efficient methods should approximate; it is a noisy baseline that includes many irrelevant interactions. Learning to focus, rather than learning to approximate, is a more productive framing for efficient attention research.

## Acknowledgments and Disclosure of Funding

We thank the anonymous reviewers for their valuable feedback. All experiments were conducted on NVIDIA H100 GPUs. The authors declare no competing interests.

## References

- Iz Beltagy, Matthew E Peters, and Arman Cohan. Longformer: The long-document transformer. *arXiv preprint arXiv:2004.05150*, 2020.
- Dan Biderman, Jacob Portes, Jose Javier Gonzalez Ortiz, Mansheej Paul, Philip Greengard, Connor Havens, Robert Jennings, Daniel King, Sam Havens, Nick Blankenship, et al. LoRA learns less and forgets less. *Transactions on Machine Learning Research*, 2024.
- Peter F Brown, Vincent J Della Pietra, Peter V deSouza, Jennifer C Lai, and Robert L Mercer. Class-based n-gram models of natural language. *Computational Linguistics*, 18(4):467–480, 1992.
- Mathilde Caron, Ishan Misra, Julien Mairal, Priya Goyal, Piotr Bojanowski, and Armand Joulin. Unsupervised learning of visual features by contrasting cluster assignments. In *Advances in Neural Information Processing Systems*, 2020.
- Krzysztof Choromanski, Valerii Likhoshesterov, David Dohan, Xingyou Song, Andreea Gane, Tamas Sarlos, Peter Hawkins, Jared Davis, Afroz Mohiuddin, Lukasz Kaiser, et al. Rethinking attention with performers. In *International Conference on Learning Representations*, 2021.
- Tri Dao. FlashAttention-2: Faster attention with better parallelism and work partitioning. In *International Conference on Learning Representations*, 2024.

- Tri Dao and Albert Gu. Transformers are SSMS: Generalized models and efficient algorithms through structured state space duality. In *International Conference on Machine Learning*, 2024.
- Tri Dao, Dan Fu, Stefano Ermon, Atri Rudra, and Christopher Ré. FlashAttention: Fast and memory-efficient exact attention with IO-awareness. In *Advances in Neural Information Processing Systems*, 2022.
- DeepSeek-AI. DeepSeek-V2: A strong, economical, and efficient mixture-of-experts language model. *arXiv preprint arXiv:2405.04434*, 2024a.
- DeepSeek-AI. DeepSeek-V3 technical report. *arXiv preprint arXiv:2412.19437*, 2024b.
- William Fedus, Barret Zoph, and Noam Shazeer. Switch transformers: Scaling to trillion parameter models with simple and efficient sparsity. *Journal of Machine Learning Research*, 23(120):1–39, 2022.
- Gemma Team. Gemma 2: Improving open language models at a practical size. *arXiv preprint arXiv:2408.00118*, 2024.
- Dirk Groeneveld, Iz Beltagy, Pete Walsh, Akshita Bhagia, Rodney Kinney, Oyvind Tafjord, Ananya Harsh Joshi, Valentina Pyatkin, et al. OLMo: Accelerating the science of language models. In *Annual Meeting of the Association for Computational Linguistics*, 2024.
- Edward J Hu, Yelong Shen, Phillip Wallis, Zeyuan Allen-Zhu, Yuanzhi Li, Shean Wang, Lu Wang, and Weizhu Chen. LoRA: Low-rank adaptation of large language models. In *International Conference on Learning Representations*, 2022.
- Albert Q Jiang, Alexandre Sablayrolles, Arthur Mensch, Chris Bamford, Devendra Singh Chaplot, Diego de las Casas, Florian Bressand, Gianna Lengyel, Guillaume Lample, Lucile Saulnier, et al. Mistral 7B. *arXiv preprint arXiv:2310.06825*, 2023.
- Albert Q Jiang, Alexandre Sablayrolles, Antoine Roux, Arthur Mensch, Blanche Savary, Chris Bamford, Devendra Singh Chaplot, Diego de las Casas, Emma Bou Hanna, Florian Bressand, et al. Mixtral of experts. *arXiv preprint arXiv:2401.04088*, 2024a.
- Huiqiang Jiang, Yucheng Li, Chengruidong Zhang, Qianhui Wu, Xufang Luo, Surin Ahn, Zhenhua Han, Amir H Abdi, Dongsheng Li, Chin-Yew Lin, et al. MInference 1.0: Accelerating pre-filling for long-context LLMs via dynamic sparse attention. In *Advances in Neural Information Processing Systems*, 2024b.
- Angelos Katharopoulos, Apoorv Vyas, Nikolaos Pappas, and François Fleuret. Transformers are RNNs: Fast autoregressive transformers with linear attention. In *International Conference on Machine Learning*, 2020.
- Jakub Krajewski, Jan Ludziejewski, Kamil Adamczewski, Maciej Piotrowski, Piotr Sankowski, Michał Ciebiera, Krystian Król, Tomasz Odrzygóźdź, Marek Jaszczur, et al. Scaling laws for fine-grained mixture of experts. In *International Conference on Machine Learning*, 2024.

- Opher Lieber, Barak Lenz, Horace Bata, Gal Cohen, Jhonathan Osin, Itay Dalmedigos, Erez Safahi, Shaked Meirum, Yonatan Belinkov, Amnon Shashua, and Yoav Shoham. Jamba: A hybrid transformer-mamba language model. *arXiv preprint arXiv:2403.19887*, 2024.
- Hao Liu, Matei Zaharia, and Pieter Abbeel. Ring attention with blockwise transformers for near-infinite context. In *International Conference on Learning Representations*, 2024a.
- Shih-Yang Liu, Chien-Yi Wang, Hongxu Yin, Pavlo Molchanov, Yu-Chiang Frank Wang, Kwang-Ting Cheng, and Min-Hung Chen. DoRA: Weight-decomposed low-rank adaptation. In *International Conference on Machine Learning*, 2024b.
- Llama Team. The llama 3 herd of models. *arXiv preprint arXiv:2407.21783*, 2024.
- Shuming Lu et al. MoBA: Mixture of block attention for long-context LLMs. *arXiv preprint arXiv:2502.13189*, 2025.
- Michael McCloskey and Neal J Cohen. Catastrophic interference in connectionist networks: The sequential learning problem. In *Psychology of Learning and Motivation*, volume 24, pages 109–165. Elsevier, 1989.
- Joan Puigcerver, Carlos Riquelme, Basil Mustafa, and Neil Houlsby. From sparse to soft mixtures of experts. In *International Conference on Learning Representations*, 2024.
- Aurko Roy, Mohammad Saffar, Ashish Vaswani, and David Grangier. Efficient content-based sparse attention with routing transformers. *Transactions of the Association for Computational Linguistics*, 9:53–68, 2021.
- Jay Shah, Ganesh Bikshandi, Ying Zhang, Vijay Thakkar, Pradeep Ramani, and Tri Dao. FlashAttention-3: Fast and accurate attention with asynchrony and low-precision. In *Advances in Neural Information Processing Systems*, 2024.
- Ashish Vaswani, Noam Shazeer, Niki Parmar, Jakob Uszkoreit, Llion Jones, Aidan N Gomez, Lukasz Kaiser, and Illia Polosukhin. Attention is all you need. In *Advances in Neural Information Processing Systems*, 2017.
- Sinong Wang, Belinda Z Li, Madian Khabsa, Han Fang, and Hao Ma. Linformer: Self-attention with linear complexity. *arXiv preprint arXiv:2006.04768*, 2020.
- An Yang, Baosong Yang, Binyuan Hui, Bo Zheng, Bowen Yu, Chang Zhou, et al. Qwen2.5 technical report. *arXiv preprint arXiv:2412.15115*, 2024.
- Hengshuai Yao and Guan Wang. Think keys: Low-dimensional query-key attention with full-dimensional values. 2025.
- Tianzhu Ye, Li Li, Gao Huang, et al. Differential transformer. In *International Conference on Learning Representations*, 2025.
- Jingyang Yuan, Huazuo Liu, Zhaozhuo Zhang, et al. Native sparse attention: Hardware-aligned and natively trainable sparse attention. In *Annual Meeting of the Association for Computational Linguistics*, 2025.

Manzil Zaheer, Guru Guruganesh, Kumar Avinava Dubey, Joshua Ainslie, Chris Alberti, Santiago Ontanon, Philip Pham, Anirudh Ravula, Qifan Wang, Li Yang, et al. Big bird: Transformers for longer sequences. In *Advances in Neural Information Processing Systems*, 2020.

Michael Zhang, Kush Bhatia, Jonathan Ragan-Kelley, and Christopher Ré. The hedgehog & the porcupine: Expressive linear attentions with softmax mimicry. In *International Conference on Learning Representations*, 2024.

## Appendix A. Background: Three Families of Efficient Attention

Standard attention computes, for each query position  $t$ :

$$\text{output}_t = \sum_{i \leq t} \frac{\exp(q_t \cdot k_i / \sqrt{d})}{\sum_{j \leq t} \exp(q_t \cdot k_j / \sqrt{d})} \cdot v_i \quad (6)$$

This requires computing  $q_t \cdot k_i$  for all  $i \leq t$ , giving  $O(T^2)$  operations. Three families of methods reduce this cost through fundamentally different strategies (Table 24).

### A.1 Sparse Attention: Keep Some Pairs, Drop Others

Sparse methods select a subset of key–value pairs for each query and apply *exact softmax* over only those pairs. Longformer (Beltagy et al., 2020) uses a fixed pattern: each query attends to a local window plus a few global tokens. BigBird (Zaheer et al., 2020) adds random attention pairs. Routing Transformer clusters tokens with online  $k$ -means and attends within clusters. MoBA (Lu et al., 2025) partitions the KV sequence into fixed-size blocks, computes a representative key per block (the mean), and routes each query to its top- $k$  blocks—applying MoE principles at block granularity rather than token granularity.

These methods preserve the attention function (exact softmax) but use *hand-designed* or *coarse-grained* rules to decide which pairs to keep. Recent work explores dynamic sparse patterns identified post-hoc in pretrained models (Jiang et al., 2024b) and hardware-aligned natively trainable sparse attention (Yuan et al., 2025). An orthogonal approach, Differential Transformer (Ye et al., 2025), promotes sparsity through architectural modification (attention as a difference of two softmax maps). When retrofitted onto pretrained models, fixed patterns may discard pairs the model learned to rely on, causing quality loss. Focus belongs to this family but *learns* which pairs to keep from data, avoiding the pattern mismatch problem.

### A.2 Linear Attention: The Kernel Trick

Linear attention methods (Katharopoulos et al., 2020; Choromanski et al., 2021; Zhang et al., 2024) replace the softmax nonlinearity with a kernel approximation. The key identity: if we define a feature map  $\phi$  such that  $\phi(q)^\top \phi(k) \approx \exp(q \cdot k / \sqrt{d})$ , then:

$$\text{output}_t = \frac{\phi(q_t)^\top \sum_{i \leq t} \phi(k_i) v_i^\top}{\phi(q_t)^\top \sum_{i \leq t} \phi(k_i)} = \frac{\phi(q_t)^\top S_t}{\phi(q_t)^\top z_t} \quad (7)$$

where  $S_t = \sum_{i \leq t} \phi(k_i)v_i^\top$  and  $z_t = \sum_{i \leq t} \phi(k_i)$  are *running sums* that can be updated incrementally:

$$S_t = S_{t-1} + \phi(k_t)v_t^\top, \quad z_t = z_{t-1} + \phi(k_t) \quad (8)$$

Each update costs  $O(m \cdot d_v)$  where  $m$  is the feature dimension, giving  $O(T \cdot m \cdot d_v)$  total—linear in sequence length.

**Why this works: associativity.** The crucial property is that without the softmax non-linearity, the sum over keys can be factored out of the query computation. With standard softmax,  $\text{softmax}(q \cdot k_1) \cdot v_1 + \text{softmax}(q \cdot k_2) \cdot v_2$  cannot be simplified because softmax couples all positions through its normalizing denominator. With the kernel decomposition,  $\phi(q)^\top \phi(k_1) \cdot v_1 + \phi(q)^\top \phi(k_2) \cdot v_2 = \phi(q)^\top [\phi(k_1)v_1^\top + \phi(k_2)v_2^\top]$ , and the bracketed sum is exactly  $S_2$ .

**The approximation cost.** Performer (Choromanski et al., 2021) uses random feature maps (FAVOR+):  $\phi(x) = \exp(Wx - \|x\|^2/2)/\sqrt{m}$  where  $W$  is a random matrix. This approximates softmax but never equals it exactly. When retrofitted onto a pretrained model that learned specific attention patterns using exact softmax, the kernel approximation destroys those patterns—analogueous to replacing a lens with one of a different prescription. This is why Performer consistently fails in the retrofit setting (Section 3.2).

**Implementation: the cumsum dilemma.** While the recurrence  $S_t = S_{t-1} + \phi(k_t)v_t^\top$  is mathematically elegant, implementing it efficiently on GPUs requires care:

1. **Iterative loop:** Compute each  $S_t$  sequentially. Memory-efficient ( $O(m \cdot d_v)$  state) but serializes  $T$  CUDA kernel launches—extremely slow on GPUs which are designed for parallel work.
2. **Full vectorization:** Materialize all outer products  $\phi(k_i)v_i^\top$  as a tensor of shape  $(T, m, d_v)$  and apply `torch.cumsum` in parallel. Fast, but stores the full  $(B, H, T, m, d_v)$  tensor—with batch size 8 and 12 heads, this exceeds 24GB and causes out-of-memory.
3. **Per-sample vectorization:** Loop over the batch dimension (small:  $B = 8$ ) while vectorizing over the sequence dimension (large:  $T = 1024$ ) using `cumsum`. This balances memory ( $1/B$  of the full tensor) with speed (parallel prefix sum within each sample).

Our comparison (Section 3.2) uses option 3 to ensure Performer runs at reasonable speed. Despite this, the quality gap remains fundamental: the kernel approximation, not the implementation, is the bottleneck.

### A.3 Low-Rank Attention: Compress Keys and Values

Linformer (Wang et al., 2020) projects keys and values from  $T$  positions to  $k \ll T$  “virtual” positions using learnable matrices  $E, F \in \mathbb{R}^{k \times T}$ :

$$\tilde{K} = E \cdot K, \quad \tilde{V} = F \cdot V, \quad \text{output} = \text{softmax}\left(\frac{Q\tilde{K}^\top}{\sqrt{d}}\right)\tilde{V} \quad (9)$$

This reduces the attention matrix from  $(T \times T)$  to  $(T \times k)$ , giving  $O(T \cdot k)$  complexity. However, the projection destroys positional structure: the  $k$  virtual positions are linear combinations of all original positions, making causal masking impossible in the standard sense. This is a fundamental limitation for autoregressive language models.

#### A.4 Where Focus Fits

Focus belongs to the sparse attention family: it selects which key–value pairs each query attends to, then applies *exact softmax* over the selected pairs. The critical difference from prior sparse methods is that the selection is *learned* from data via centroid routing, rather than determined by fixed positional patterns.

This choice has two consequences. First, the attention computation within each group is *identical* to what the pretrained model learned—no approximation, no projection, no kernel trick. This is why retrofit works: the model’s learned attention patterns are preserved on the pairs that matter most. Second, the sparsity pattern adapts to the data: Focus can discover that pronouns should attend to nouns, or that punctuation can safely ignore distant content words, without hand-designed rules.

Family	Exact softmax?	Pattern	Retrofit?	Complexity
Sparse (Longformer)	Yes	Fixed	Poor	$O(T \cdot w)$
Linear (Performer)	No — kernel approx	All pairs	Fails	$O(T \cdot m \cdot d)$
Low-rank (Linformer)	On compressed pairs	All $\rightarrow k$	Poor	$O(T \cdot k)$
<b>Ours</b>	<b>Yes</b>	<b>Learned</b>	<b>Works</b>	$O(T^2/K)$

Table 24: Three families of efficient attention and where Focus fits. Only Focus combines exact softmax with learned sparsity.

## Appendix B. Related Work

### B.1 Relationship to Routing Transformers

Our closest prior work is Routing Transformers (Roy et al., 2021), which also uses content-based clustering to determine which token pairs attend to each other. Both methods share the core insight that *data-driven* sparsity patterns outperform fixed patterns (local windows, strided patterns) because different inputs require attention between different token pairs.

The approaches diverge in three consequential ways:

	Routing Transformer	Focus
Clustering	Online $k$ -means (per step)	Learned centroids (converged)
Assignment	Hard (argmin)	Soft (Sinkhorn-balanced)
Integration	Replaces attention mask	Gates existing attention
Training	From scratch only	Retrofits onto pretrained
Balancing	None	Sinkhorn normalization

**Learned vs. transient clusters.** Routing Transformers re-cluster queries and keys with online  $k$ -means at every forward pass—different random initialization, different clusters each

step and each layer. This has two consequences: (1) clusters carry no semantic continuity across steps, making it difficult for the model to learn to *rely* on cluster membership, and (2) the per-step clustering cost ( $O(nKd)$  with  $K$  clusters) cannot be amortized. Our centroids are learned parameters that converge during training, producing stable semantic categories (pronouns, prepositions, content words; Section 4) that persist at inference with zero per-step cost.

**Gating vs. masking.** Routing Transformers replace the attention mask entirely: a query attends *only* to keys in its cluster (plus a local window). This is a hard decision—if a token is assigned to the wrong cluster, the relevant key is invisible. Our method *gates* attention weights multiplicatively: the pretrained attention pattern is preserved in full within the local window, and modulated softly beyond it. This distinction is critical for retrofitting: gating starts near identity (all pairs allowed) and gradually learns which distant pairs to suppress, whereas replacing the mask immediately disrupts the pretrained attention patterns.

**Training stability.** Without explicit balancing, Routing Transformers are susceptible to the group dominance pathways we identify in Section 3.6: one cluster can absorb most tokens, leaving other clusters with too few keys to form useful attention patterns. Our Sinkhorn normalization enforces balanced assignment as a hard constraint, which we show is necessary for convergence (Section 3.6).

We include Routing Transformers in our unified retrofit comparison (Section 3.2), where the differences between transient and learned clustering become empirically measurable. Online  $k$ -means routing achieves 37.4 PPL in the retrofit setting—better than fixed-pattern methods (Longformer: 38.9) but worse than learned centroids (36.0)—confirming that content-based routing is a sound principle while stable, learned clusters outperform transient ones.

## B.2 Relationship to MoBA

MoBA (Mixture of Block Attention) (Lu et al., 2025) applies MoE principles to attention by partitioning the KV sequence into fixed-size blocks, computing a mean key per block as its representative, and routing each query to the top- $k$  blocks via this coarse similarity score. Within selected blocks, exact softmax attention is computed—preserving the attention function, as in Focus. MoBA has been deployed in Kimi’s long-context system, demonstrating practical viability.

Despite the shared MoE-for-attention motivation, Focus and MoBA differ in three important ways:

	MoBA	Focus
Routing granularity	Block-level (mean key)	Token-level (learned centroids)
Routing parameters	None (uses existing keys)	Learned centroids (148K params)
Sparsity pattern	Input-dependent blocks	Learned semantic groups
Training setting	From scratch	Retrofit or from scratch
Quality vs. full attention	Matches	Surpasses

**Block vs. token granularity.** MoBA’s block-level routing selects *contiguous chunks* of keys for each query: all tokens in a selected block are attended to, and all tokens in a

non-selected block are ignored. This coarse granularity is hardware-friendly but cannot distinguish semantically relevant tokens from irrelevant ones within the same block. Focus routes at token granularity—two tokens attend to each other if and only if they share a semantic group, regardless of their positions. This finer granularity is what enables Focus to *surpass* full attention: it filters irrelevant token pairs that block-level methods must retain.

**Learned vs. parameter-free routing.** MoBA requires no additional parameters—it routes based on the mean of existing keys. This is elegant for from-scratch training where the model co-adapts its keys to produce useful block-level summaries. However, this means MoBA cannot be retrofitted onto a pretrained model without retraining: the pretrained keys were not trained to be block-summarizable. Focus adds a small set of learned centroids that adapt to the pretrained model’s representations, enabling retrofit with zero benchmark degradation.

**Complementary strengths.** MoBA’s hardware-aligned block structure and Focus’s semantic token-level routing address different regimes. MoBA is well-suited for extremely long contexts where block-level approximation suffices and hardware efficiency dominates. Focus targets settings where quality improvement and retrofit capability are paramount. The two approaches could potentially be combined: Focus’s learned groups could select which blocks to attend within, providing both semantic precision and hardware alignment.

Mixture of Experts (MoE) (Fedus et al., 2022; Jiang et al., 2024a; DeepSeek-AI, 2024a) and Focus both use learnable parameters to direct computation and face similar training challenges (Section 3.6), but serve fundamentally different purposes:

	MoE	Focus
Directs	FFN computation	Attention connections
Groups mean	“Process similarly”	“Semantically related”
Interaction	Token $\rightarrow$ Expert (independent)	Token $\leftrightarrow$ Token (direct)
Saves	FFN compute	Attention compute

MoE tokens routed to the same expert never interact—they are processed independently by the same FFN. Our groups explicitly create *attention paths* between distant tokens. The two approaches are complementary: MoE routes computation, Focusing directs communication. Recent advances in MoE routing—including auxiliary-loss-free balancing (DeepSeek-AI, 2024b), soft mixtures (Puigcerver et al., 2024), and fine-grained scaling laws (Krajewski et al., 2024)—address the load-balancing problem from the FFN side; our Sinkhorn normalization solves the analogous problem for attention routing.

### B.3 Relationship to Thin Keys: A Unified Selection Dimension View

Thin Keys (Yao and Wang, 2025) and Focus are complementary selection mechanisms operating at different granularities:

	Thin Keys	Focus
Selection level	Token-level (fine)	Group-level (coarse)
Mechanism	Compressed QK matching	Centroid affinity gating
Reduces	Per-pair cost ( $d_k$ )	Number of pairs evaluated

**The  $d_{\text{select}}$  abstraction.** The core finding of Thin Keys is that query-key dimensions can be compressed far below value dimensions ( $d_k \ll d_v$ ) without quality loss, because *selection requires less capacity than transfer*. Focus reveals the same principle at a coarser level: the group projection  $W_g \in \mathbb{R}^{d \times d_g}$  maps tokens into a  $d_g$ -dimensional space for centroid matching.

Both mechanisms project into a low-dimensional *selection space*; they differ only in what is being selected:

Selection stage	Dimension	Question answered	Output
Group routing (this work)	$d_g \approx 16$	“Which <i>kind</i> of token?”	Binary: same group / different group
Token matching (Thin Keys)	$d_k \ll d$	“Which <i>specific</i> token?”	Soft: attention weight per token
Content transfer (standard)	$d_v = d$	“What information to read?”	Dense: value vector

This suggests a general principle: **attention is a hierarchy of progressively finer selection stages, each requiring progressively more dimensions:**

$$d_g \ll d_k \ll d_v = d \tag{10}$$

**Why  $d_g \ll d_k$ : decision complexity determines dimensionality.** Group routing answers a *categorical* question: “is this token a pronoun, a preposition, punctuation, or a content word?” With  $K = 8$  groups, this is a classification into  $K$  categories requiring at most  $K - 1 = 7$  discriminative dimensions. Token matching answers a *discriminative* question: “among hundreds of candidate tokens in my group, which specific one is relevant right now?” This requires far more capacity. An analogy: group routing is sorting mail by zip code; token matching is finding a specific letter within a mailbag.

**Compound efficiency from hierarchical selection.** Combining both mechanisms creates a two-stage pipeline:

$$\underbrace{\text{Focus}}_{\text{reduces pairs: } O(n^2) \rightarrow O(n \cdot n/K)} \quad \circ \quad \underbrace{\text{Thin Keys}}_{\text{reduces per-pair cost: } d \rightarrow d_k} \tag{11}$$

The total cost becomes  $O(n \cdot (n/K) \cdot d_k)$ , achieving savings along both axes simultaneously. For concrete parameters ( $n = 4096$ ,  $K = 8$ ,  $d_k = d/4$ ), this yields a  $\sim 32\times$  reduction in distant attention compute versus standard  $O(n^2 \cdot d)$ . The two mechanisms are *structurally complementary*: Focus solves the *candidate set* problem, while Thin Keys solves the *fine selection* problem. We leave empirical combination in a single model to future work.

## Appendix C. Ablation Studies

Table 25 ablates four key hyperparameters on GPT-2 124M / PG-19, varying each while holding others at defaults ( $K=8$ ,  $w=128$ ,  $\tau=0.1$ , Sinkhorn iters=10).

**Fine-tuned PPL is robust.** Across all 16 configurations, fine-tuned PPL ranges from 29.9 to 30.5 — a spread of only 0.6 PPL. The method is not sensitive to hyperparameter choices.

Parameter	Value	Centroid PPL	Fine-tuned PPL	Max grp P1	Max grp P2
Groups $K$	4	36.8	<b>30.1</b>	40%	38%
	8	38.4	30.3	24%	23%
	16	40.4	30.4	20%	31%
	32	42.4	30.5	21%	30%
Window $w$	64	38.3	30.2	17%	17%
	128	38.4	30.2	26%	23%
	256	38.1	30.3	26%	25%
	512	38.6	<b>30.0</b>	27%	28%
Temp $\tau$	0.05	<b>36.9</b>	<b>30.0</b>	68%	74%
	0.1	38.4	30.3	24%	23%
	0.2	39.1	30.3	16%	19%
	0.5	40.5	30.3	21%	31%
Sinkhorn iters	3	35.8	29.9	95%	97%
	5	36.8	30.2	69%	75%
	10	38.4	30.3	21%	20%
	20	39.0	30.2	14%	14%

Table 25: Ablation study (GPT-2 124M, PG-19). Each row varies one hyperparameter with others at defaults ( $K=8$ ,  $w=128$ ,  $\tau=0.1$ , 10 Sinkhorn iters). Fine-tuned PPL is stable (29.9–30.5) across all 16 configurations.

**Sinkhorn iterations: a subtle trap.** With 3 iterations, PPL appears best (29.9) but groups have collapsed to 95–97% dominance. This is not real Focus — it is effectively full attention with extra overhead. At low temperature ( $\tau=0.1$ ), the exponential  $\exp(\text{scores}/0.1)$  produces extremely peaked distributions that 3 iterations cannot redistribute. At least 10 iterations are needed to maintain balanced groups (20% max), and 20 iterations provide only marginal additional balance (14% max).

**Temperature controls the balance–sharpness tradeoff.**  $\tau=0.05$  achieves the best centroid-only PPL (36.9) but with 68–74% max group, indicating partial collapse.  $\tau=0.1$  balances sharp assignments with group balance. Higher temperatures ( $\tau \geq 0.2$ ) produce well-balanced but softer assignments.

**Window size: smaller is better.** We sweep the local window size  $w$  with  $K=2$ , centroid-only, 2000 steps:

$w=64$	$w=128$	$w=256$	$w=512$
<b>34.1</b>	34.6	35.3	37.5

Larger windows degrade quality:  $w=512$  (half the sequence) performs worst because most attention is handled locally, leaving little for the learned groups to contribute. Smaller windows force the model to rely on group-routed long-range attention, which is more selective and effective. This reinforces the central finding: restricting attention to relevant tokens outperforms attending broadly.

**Group count  $K$  with extended training.** To confirm the effect of group count under longer training (4000 fine-tuning steps), we re-ran the  $K$  ablation with Sinkhorn:

Groups $K$	Full FT	Local FT	Focus FT	$\Delta$ vs Full
2	29.3	34.0	<b>29.4</b>	+0.1
4	29.3	33.9	29.7	+0.4
8	29.3	33.6	30.0	+0.7
16	29.3	33.6	30.0	+0.7

Fewer groups consistently perform better:  $K=2$  achieves the lowest PPL (29.4—only 0.1 from full attention). The gate signal strengthens dramatically with fewer groups: mean gate rises from 0.548 ( $K=16$ ) to 0.646 ( $K=4$ ) to 0.806 ( $K=2$ ), with 67% of gates above 0.8 at  $K=2$ . This monotonic trend reveals that the method benefits from the coarsest possible partition: just splitting tokens into two semantic categories suffices to capture the relevant structure.

**Cross-dataset validation with  $K=4$ .** On Wikitext-103 with  $K=4$ , Focus *exceeds* full attention (21.2 vs 21.7 PPL), replicating the quality improvement observed on PG-19 at 124M. Restricting attention helps most when the model is prone to overfitting on irrelevant attention paths.

**Best configuration: fewer groups, longer training.** Combining coarse grouping with extended training yields near-parity with full attention. The trend holds at all three scales:

Scale	Config	FT steps	Full FT	Focus FT	Gap
124M	$K=8$	2,000	29.4	29.7	0.3
124M	$K=8$	8,000	26.6	26.8	0.2
124M	$K=2$	4,000	29.3	29.4	0.1
774M	$K=8$	4,000	19.7	20.3	0.6
774M	$K=2$	4,000	19.7	19.8	0.1
1.5B	$K=8$	4,000	19.3	19.7	0.4
1.5B	$K=2$	4,000	19.0	<b>19.2</b>	<b>0.2</b>

At every scale, fewer groups outperform more groups.  $K=2$  is within 0.1–0.2 PPL of full attention at all scales. However, there is a clear *PPL–interpretability tradeoff*:  $K=2$  groups are opaque (half the tokens in each bucket with no discernible semantic pattern),  $K=4$  produces rough but recognizable categories (structural markers, content words), and  $K=8$  yields clean linguistic categories (pronouns, determiners, punctuation separate cleanly). We recommend  $K=4$  as the practical default—it achieves near-parity (0.1–0.3 PPL gap) while maintaining interpretable group structure.

This yields a practical recommendation: *use the fewest groups that maintain meaningful semantic categories, with longer training.*

**Window size: smaller is better.** With learned group routing handling long-range dependencies, the local window needs only to capture immediate context. We ablate window size with  $K=2$  centroid-only training (2000 steps):

$w$	8	<b>16</b>	32	64	128	256	512
PPL	33.9	<b>33.8</b>	34.0	34.1	34.6	35.3	37.5

Smaller windows consistently outperform larger ones:  $w=16$  achieves the best PPL (33.8), beating the default  $w=128$  by 0.8 PPL, with diminishing returns below  $w=16$ . At  $w=512$ , the local window already covers half the sequence, leaving little for group routing to contribute—quality drops by 3.7 PPL. This confirms that local and group attention are complementary: the local window handles nearby syntax, while learned groups handle distant semantics. The model needs only 16 tokens of local context when group routing provides long-range access.

To quantify the value of group routing, we compare against a local-only baseline at  $w=32$ : local attention alone achieves 45.7 PPL even after 4000 steps of fine-tuning, while adding centroid-only groups brings this to 34.0—an 11.7 PPL improvement from routing alone, without touching any model weights.

**Centroid training converges fast.** We train  $K=2$  centroids for up to 32K steps to characterize the convergence curve:

Steps	2000	4000	8000	16000	32000
PPL	34.6	<b>34.1</b>	34.4	34.4	34.3

Centroid training reaches its optimum at 4000 steps and plateaus thereafter. This is expected: the routing decision (“which group?”) is a simple classification that converges quickly. Practical recommendation: 4000 centroid training steps suffice regardless of model scale.

## Appendix D. Extended Training Results

Our main results use 2000 centroid + 2000 fine-tuning steps. To test whether the remaining gap closes with more compute, we extended fine-tuning on GPT-2 124M / PG-19 to 8000 steps (Table 26):

FT steps	Full FT	Local FT	Focus FT	Gap
2,000	29.4	32.7	29.7	0.3
4,000	28.0	31.2	28.3	0.3
8,000	26.6	29.4	26.8	0.2

Table 26: Longer training narrows the gap (GPT-2 124M, PG-19). At 8000 steps, Focus (26.8) is within 0.2 PPL of full attention (26.6).

The absolute PPL of all methods improves substantially (full attention drops from 29.4 to 26.6), yet Focus tracks this improvement closely, maintaining a gap of only 0.2 PPL at 8000 steps. The gap is not an architectural ceiling but a training dynamics effect. Groups remain balanced and semantically coherent throughout extended training, with maximum group size at 29%—confirming that Sinkhorn’s structural constraint does not degrade with longer optimization.

**Extended training at larger scales.** We also extended training to 8000 steps at 774M and 1.5B ( $K=8$ ):

Scale	FT steps	Full FT	Focus FT	Gap
124M	2,000	29.4	29.7	0.3
124M	8,000	26.6	26.8	0.2
774M	4,000	19.7	20.3	0.6
774M	8,000	19.3	19.6	0.3
1.5B	4,000	19.3	19.7	0.4
1.5B	8,000	18.7	19.1	0.4

At 774M, the gap halves from 0.6 to 0.3 PPL with extended training, mirroring the 124M trajectory. At 1.5B, the gap holds at 0.4 PPL. At all scales, Focus is within 0.2–0.4 PPL of full attention with 8000 steps, suggesting that the remaining gap may close further with  $K=2$  groups (Appendix C) or input-dependent centroids.

## Appendix E. Additional Discussion

### E.1 Focus as an Additive Capability

An alternative view of Focus—complementary to the structural constraint perspective—is that it adds a *missing capability* to existing pretrained transformers. A standard transformer can read every token in its context but has no mechanism to determine, before computing attention, which tokens are worth reading at distance. It evaluates all  $n^2$  pairs and relies on softmax to sort signal from noise post hoc. This is analogous to reading an entire book to find one relevant paragraph, rather than first consulting the index.

Focus adds the index. The centroid-only model (Phase 1:  $\sim 7$ M centroid parameters trained, all 124M pretrained weights frozen) learns to classify tokens by semantic role and route attention accordingly—without modifying the model’s existing knowledge or capabilities. On standard benchmarks (HellaSwag, ARC-Easy, PIQA, LAMBADA), the centroid-only model matches the unmodified pretrained model with zero measurable degradation (Table 5), confirming that focus is purely additive: it provides new routing structure without degrading existing function.

**Connection to catastrophic forgetting.** This result is notable in the context of continual learning, where fine-tuning on new data typically degrades performance on previous tasks—the well-known problem of catastrophic forgetting (McCloskey and Cohen, 1989). Standard fine-tuning of all model parameters creates interference between old and new knowledge because they occupy the same parameter space. On PG-19, full fine-tuning improves domain PPL dramatically ( $42.8 \rightarrow 31.4$ ) but destroys general capabilities: LAMBADA accuracy drops from 32.6% to 9.4%, a loss of 23.2 percentage points (Table 7).

Centroid-only training avoids this entirely: the centroid parameters occupy a *separate* parameter space from the model’s knowledge (attention weights, FFN weights, embeddings). They cannot interfere because they encode a different kind of information—routing structure rather than factual knowledge. The result is strictly better than the pretrained model: PG-19 PPL improves ( $42.8 \rightarrow 34.2$ ) while all general benchmarks remain unchanged. This is

the ideal outcome that continual learning methods strive for but rarely achieve cleanly: *domain-specific gain with zero cross-task interference*.

The centroids learn universal linguistic categories (pronouns, prepositions, content words) that transfer across domains: centroids trained on PG-19 (19th century books) produce identical downstream benchmark performance as centroids trained on WikiText-103 (encyclopedic text), because part-of-speech structure is domain-invariant (Table 8).

This has a practical implication: Focus can be deployed as a lightweight post-training add-on to any pretrained transformer. The centroid parameters ( $\sim 7\text{M}$  for 124M,  $\sim 59\text{M}$  for 774M,  $\sim 123\text{M}$  for 1.5B) train in minutes on a single GPU and require no modification to the pretrained weights. The centroid parameter count is dominated by the  $d \times d$  projection in each layer; a low-rank projection ( $d \rightarrow d_g$  with  $d_g \ll d$ ) would reduce this substantially, consistent with our finding that selection is inherently low-dimensional (Appendix B.3). The model gains the ability to focus its attention—and with it, both quality improvements (at smaller scales) and efficiency gains (via thresholded inference)—at negligible cost.

## E.2 Learning to Focus vs Approximating Attention

The efficient attention literature has largely treated the problem as one of *approximation*: given that full attention computes  $n^2$  interactions, how can we approximate this computation with fewer operations? Longformer uses fixed local + global patterns. Linformer projects keys and values to lower rank. Performer uses random feature maps to approximate the softmax kernel.

These approaches assume the full attention matrix is the target to be recovered. Our results challenge this assumption. If restricting attention to semantically relevant pairs *improves* quality, then the full attention matrix is not the right target—it contains noise that actively hurts performance. The  $n^2$  interactions are not all signal; many are distractors.

This suggests a different research direction: rather than approximating full attention, *learn which attention pairs matter*. The problem shifts from numerical linear algebra (low-rank approximation, kernel methods) to representation learning (what makes two tokens relevant to each other?). Our semantic groups are one answer; there may be others. The key insight is that the question itself has changed: not “how to compute attention cheaply” but “what should attention compute at all.”

**Complementary perspectives, not opposing ones.** Framing efficient attention as a learning problem does not place our method outside the efficient attention literature—it provides a different lens on the same goal. The sparsity pattern our method learns is *also* a valid approximation of full attention, and can be evaluated as such. The distinction is in how the pattern is derived: fixed heuristics (Longformer’s sliding window, BigBird’s random blocks), mathematical structure (Linformer’s low-rank projection, Performer’s kernel approximation), or data-driven learning (our approach). The learned pattern achieves a better quality–efficiency tradeoff not because learning is inherently superior to approximation, but because the specific question—*which token pairs share semantic relevance?*—is better answered by learning from data than by structural assumptions.

**Comparison with efficient attention methods.** Table 27 positions our method within the efficient attention landscape. We compare along four axes: how the sparsity pattern

is determined, the asymptotic complexity, whether the method can be retrofitted onto pretrained models, and the quality–efficiency tradeoff.

Method	Pattern source	Complexity	Retrofit?	Quality impact
Full attention	—	$O(n^2)$	—	Baseline
Longformer	Fixed (local + global)	$O(n)$	Degrades (+3.3 PPL)	Moderate loss
BigBird	Fixed (local + global + random)	$O(n)$	Not tested	Moderate loss
Performer	Kernel approximation	$O(n)$	Fails (above pretrained)	Significant loss
Linformer	Low-rank projection	$O(n)$	Degrades	Degrades on long seq
Routing Transformer	Online $k$ -means	$O(n \cdot n/K)$	Not tested	Moderate loss
MoBA	Block mean-key routing	$O(n \cdot n \cdot k/B)$	Not tested	Matches full
<b>Ours (<math>K=2</math>)</b>	<b>Learned (data-driven)</b>	$O(n^2/K)$	<b>Yes (−2.4 PPL)</b>	<b>Improves over full</b>

Table 27: Comparison with efficient attention methods. Only our method improves quality upon retrofit, preserving exact softmax while learning sparsity from data.

Several distinctions are worth noting. First, fixed-pattern methods (Longformer, Big-Bird) were originally designed for training from scratch with their sparse masks baked into the architecture. When retrofitted onto pretrained models, they degrade quality significantly (+3–4 PPL) because the fixed patterns discard attention pairs the model learned to use. Our method retrofits successfully because it preserves exact softmax on learned pairs—the pretrained computation is unchanged within each group.

Second, kernel-based approximations (Performer) struggle on long-range benchmarks. On PG-19, Performer’s trigonometric softmax approximation becomes unstable, and even positive feature maps plateau at inferior perplexity (Choromanski et al., 2021). Our method maintains or *improves* quality precisely because it does not approximate the attention function itself—it selects which inputs the attention function operates on, leaving the softmax computation exact within each group.

**Relationship to Routing Transformers and MoBA.** The closest prior works are Routing Transformers (Roy et al., 2021) and MoBA (Lu et al., 2025), which also use content-based routing to sparsify attention. Routing Transformers apply online  $k$ -means to queries and keys at each forward pass, re-clustering every step; MoBA partitions the KV sequence into fixed blocks and routes queries to top- $k$  blocks based on mean-key similarity. Our centroids are *learned parameters* that converge during training and remain fixed at inference—no per-step clustering cost, and the groups are stable across inputs. Routing Transformers do not address training stability and are vulnerable to the same group dominance pathways we identify in Section 3.6; MoBA inherits stability from its block structure but sacrifices token-level precision. Our Sinkhorn normalization provides a principled solution that maintains balanced, semantically coherent groups throughout training. Both Routing Transformers and MoBA are designed for training from scratch; our method retrofits onto existing pretrained models in a few thousand steps, which is a significant practical advantage given the cost of modern pretraining (see Section B.2 for a detailed comparison with MoBA). The shared insight—that content-based routing outperforms fixed patterns—reinforces our central claim, while our contributions (learned stable centroids, Sinkhorn balancing, retrofit capability) address the practical barriers that have limited adoption of content-based sparse attention.

Third, our compute reduction scales with  $K$ : with  $K=4$  groups, distant attention operates on  $\sim 25\%$  of token pairs; with  $K=2$ ,  $\sim 50\%$ . This is less aggressive than the  $O(n)$  complexity of Longformer or Performer, but the quality–efficiency tradeoff is far more favorable. At 774M parameters, we lose 0.1 PPL for a 3–4 $\times$  reduction in attention operations—a regime where fixed-pattern methods would lose substantially more quality, and kernel methods may not converge at all.

### E.3 Group Dominance as a General Problem

Group dominance may affect any architecture where: (a) routing and computation share representations, and (b) the task objective benefits from maximizing connectivity. This includes not only attention focusing but potentially graph neural network edge prediction, sparse mixture models, and dynamic network architectures.

The three-pathway analysis (centroid drift, representational bypass, projection bypass) generalizes beyond our setting. Any soft routing mechanism that reads from shared hidden states is vulnerable to the same instability. Our finding that *hard constraints* (Sinkhorn) succeed where *soft losses* (balance penalties) fail may apply broadly.

### E.4 Efficient Inference via FlashAttention Decomposition

During training, Focus uses soft gating: every token pair  $(i, j)$  receives a continuous gate value, requiring the full  $O(n^2)$  attention computation. At inference time, we replace soft gates with hard group assignments, yielding a sparse attention pattern that can be served by standard FlashAttention calls with no custom CUDA kernels. This section details the decomposition, explains why the naive approach fails, and presents the exact solution.

#### E.4.1 THE ATTENTION MASK UNDER HARD ASSIGNMENT

With hard group assignment (each token assigned to exactly one group), the Focus attention mask is:

$$\mathcal{M}(i, j) = \mathbf{1}[j \leq i] \wedge \left( \mathbf{1}[g(i) = g(j)] \vee \mathbf{1}[i - j \leq w] \right) \quad (12)$$

where  $g(i)$  is the group assignment of token  $i$  and  $w$  is the local window size. In words: query  $i$  attends to key  $j$  if  $j$  is causally before  $i$  and either (a)  $i$  and  $j$  are in the same group, or (b)  $j$  is within the local window.

We wish to decompose this mask into two parts, each computable by a single FlashAttention call.

#### E.4.2 THE OVERLAP PROBLEM

The natural decomposition is:

$$\mathcal{S} = \{(i, j) : j \leq i \wedge g(i) = g(j)\} \quad (\text{same-group causal}) \quad (13)$$

$$\mathcal{L} = \{(i, j) : j \leq i \wedge i - j \leq w\} \quad (\text{local window}) \quad (14)$$

so that  $\mathcal{M} = \mathcal{S} \cup \mathcal{L}$ .

The problem:  $\mathcal{S}$  and  $\mathcal{L}$  *overlap*. Token pairs that are both in the same group and within the local window appear in both sets. If we compute attention independently over  $\mathcal{S}$  and

$\mathcal{L}$  and merge via logsumexp, the overlapping pairs are **double-counted**—their attention scores contribute to both logsumexp terms, inflating their weight relative to the reference computation.

**Why subtraction fails.** One might try computing  $\mathcal{S}$  and  $\mathcal{L}$  separately and subtracting the overlap  $\mathcal{S} \cap \mathcal{L}$  in logsumexp space. This requires the “log-subtract-exp” operation:

$$\text{LSE}(\mathcal{S} \cup \mathcal{L}) = \log\left(\exp(\text{LSE}(\mathcal{S})) + \exp(\text{LSE}(\mathcal{L})) - \exp(\text{LSE}(\mathcal{S} \cap \mathcal{L}))\right) \quad (15)$$

This is numerically catastrophic: the subtraction can produce negative arguments to  $\log(\cdot)$ , especially when the overlap dominates both terms (which it does at short distances where most same-group pairs are local). We confirmed empirically that this approach produces cosine similarity of only 0.79 against the reference—far too inaccurate.

#### E.4.3 THE DISJOINT DECOMPOSITION

The key insight is to split  $\mathcal{M}$  into two sets that are **disjoint by construction**:

$$\mathcal{A} = \{(i, j) : j \leq i \wedge g(i) = g(j)\} \quad (\text{same-group causal, all distances}) \quad (16)$$

$$\mathcal{B} = \{(i, j) : j \leq i \wedge i - j \leq w \wedge g(i) \neq g(j)\} \quad (\text{cross-group local}) \quad (17)$$

**Theorem 1 (Exact decomposition)**  $\mathcal{A}$  and  $\mathcal{B}$  satisfy:

1.  $\mathcal{A} \cap \mathcal{B} = \emptyset$  (*disjoint:  $\mathcal{A}$  requires same group,  $\mathcal{B}$  requires different group*)
2.  $\mathcal{A} \cup \mathcal{B} = \mathcal{M}$  (*complete: every pair in  $\mathcal{M}$  is either same-group or cross-group-local*)

**Proof** Disjointness is immediate:  $\mathcal{A}$  requires  $g(i) = g(j)$ ,  $\mathcal{B}$  requires  $g(i) \neq g(j)$ .

For completeness: let  $(i, j) \in \mathcal{M}$ . Then  $j \leq i$  and either  $g(i) = g(j)$  or  $i - j \leq w$ . If  $g(i) = g(j)$ :  $(i, j) \in \mathcal{A}$ . If  $g(i) \neq g(j)$ : then we must have  $i - j \leq w$ , so  $(i, j) \in \mathcal{B}$ . ■

Because  $\mathcal{A}$  and  $\mathcal{B}$  partition  $\mathcal{M}$ , the merge via logsumexp is **mathematically exact**—no double-counting, no subtraction, no numerical instability.

#### E.4.4 COMPUTING SET $\mathcal{A}$ : SAME-GROUP CAUSAL ATTENTION

Set  $\mathcal{A}$  contains all same-group causal pairs at any distance. We sort tokens by group assignment (stable sort preserves causal order within each group), then reshape into  $K$  independent sequences:

1. **Sort:** Compute  $\pi = \text{argsort}(g)$  with stable sort. Tokens within the same group retain their original causal order.
2. **Pad:** Sinkhorn produces approximately balanced groups, but exact sizes vary (e.g., 132 and 124 for  $K=2, T=256$ ). We pad each group to  $\max_k |\mathcal{G}_k|$  with zero vectors (see below for correctness).
3. **FlashAttention:** Call `flash_attn_func` with `causal=True` on the padded tensor of shape  $(B \cdot K, \max_k |\mathcal{G}_k|, H, d)$ .

4. **Extract:** Gather real token outputs, discard padding positions.
5. **Unsort:** Apply  $\pi^{-1}$  to restore original token order.

**Why pad-to-max is correct.** Zero-padded dummy tokens occupy the tail positions  $n_k$  through  $\max_k |\mathcal{G}_k| - 1$  of each group (after sorting). With `causal=True`, query  $i$  attends only to keys  $j \leq i$ . Real tokens at positions 0 through  $n_k - 1$  never see dummy tokens at later positions. Dummy queries attend to real tokens (producing garbage output), but we discard these via the extract step.

**Overhead.** The padding overhead is  $(K \cdot \max_k |\mathcal{G}_k| - T)/T$ , typically 3–9% with Sinkhorn-balanced groups.

**Complexity.** Each group has  $\sim T/K$  tokens, so FlashAttention computes  $K$  blocks of  $(T/K)^2/2$  pairs (the  $/2$  from causal masking), totaling  $T^2/(2K)$  operations—a  $K \times$  reduction.

#### E.4.5 COMPUTING SET $\mathcal{B}$ : CROSS-GROUP LOCAL ATTENTION

Set  $\mathcal{B}$  contains cross-group pairs within the local window. For each query at position  $i$  in group  $g$ , we attend to keys at positions  $[i-w, i]$  that are in a *different* group. This is computed with a single masked attention over the local window:

1. **Extract local keys:** For each query position  $i$ , gather keys and values at positions  $\max(0, i-w)$  through  $i$ , producing a  $(T \times (w+1))$  key/value window (with zero-padding at sequence boundaries).
2. **Cross-group mask:** Set  $\text{mask}(i, j) = \mathbf{1}[g(i) \neq g(j)] \wedge \mathbf{1}[j \geq 0]$ . Masked positions receive  $-\infty$  before softmax.
3. **Compute attention:** Standard softmax attention over the  $(w+1)$  local keys per query.

**Edge case.** When a query has *no* cross-group keys in its window (all local tokens share its group), all scores are  $-\infty$  and softmax produces  $0/0 = \text{NaN}$ . We replace NaN weights with zero, and the logsumexp for this query is  $-\infty$ , giving it zero weight in the merge—set  $\mathcal{A}$  alone determines the output, which is correct.

**Complexity.**  $O(T \cdot w)$ , identical to standard sliding-window attention. At  $T=1\text{M}$ ,  $w=128$ :  $\sim 5$  ms versus  $\sim 1.5$  s for set  $\mathcal{A}$ . Set  $\mathcal{B}$  is never the bottleneck.

#### E.4.6 LOGSUMEXP MERGE

Given outputs and logsumexp values from both sets:

$$(\mathbf{o}_A, \ell_A) \leftarrow \text{FlashAttn}(\mathcal{A}) \tag{18}$$

$$(\mathbf{o}_B, \ell_B) \leftarrow \text{CrossGroupLocal}(\mathcal{B}) \tag{19}$$

where  $\ell_A, \ell_B \in \mathbb{R}^{B \times H \times T}$  are the per-query logsumexp values (i.e.,  $\ell_A[i] = \log \sum_{j \in \mathcal{A}_i} \exp(s_{ij})$ ), the exact merged output is:

$$\mathbf{o}[i] = \frac{e^{\ell_A[i]} \cdot \mathbf{o}_A[i] + e^{\ell_B[i]} \cdot \mathbf{o}_B[i]}{e^{\ell_A[i]} + e^{\ell_B[i]}} \quad (20)$$

For numerical stability, we subtract  $m = \max(\ell_A, \ell_B)$ :

$$\mathbf{o}[i] = \frac{e^{\ell_A[i]-m} \cdot \mathbf{o}_A[i] + e^{\ell_B[i]-m} \cdot \mathbf{o}_B[i]}{e^{\ell_A[i]-m} + e^{\ell_B[i]-m}} \quad (21)$$

When  $\ell_B[i] = -\infty$  (no cross-group local keys),  $e^{-\infty-m} = 0$  and  $\mathbf{o}[i] = \mathbf{o}_A[i]$ —the merge degrades gracefully.

**Theorem 2 (Exactness)** *The merge in Equation 20 is mathematically identical to computing softmax attention over  $\mathcal{M} = \mathcal{A} \cup \mathcal{B}$ , because  $\mathcal{A} \cap \mathcal{B} = \emptyset$ .*

**Empirical verification.** We compare the fast implementation against the  $O(T^2)$  reference at all tested configurations. Results:

$T$	$K$	$w$	Cosine Similarity	Relative Error	Groups Balanced?
128	2	64	1.0000	0.0%	Yes
256	4	64	1.0000	0.0%	Yes
512	8	64	1.0000	0.0%	Yes
128	2	64	1.0000	0.0%	No (70/58)
256	4	64	1.0000	0.0%	No (70/60/66/60)
128	4	64	1.0000	0.0%	No (40/30/28/30)

All configurations achieve cosine similarity 1.0000 against the reference, confirming mathematical exactness. The small residual errors (below the displayed precision) arise from float16 quantization in FlashAttention, not from the decomposition itself.

#### E.4.7 ALGORITHM SUMMARY

---

**Algorithm 2** Focus Inference via FlashAttention Decomposition

---

- Require:**  $\mathbf{Q}, \mathbf{K}, \mathbf{V} \in \mathbb{R}^{B \times T \times H \times d}$ , group assignments  $g \in \{0, \dots, K-1\}^{B \times T}$ , window  $w$
- 1:  $\pi \leftarrow \text{stable\_argsort}(g)$  {Sort by group, preserve causal order}
  - 2:  $\mathbf{Q}_s, \mathbf{K}_s, \mathbf{V}_s \leftarrow \text{gather}(\mathbf{Q}, \mathbf{K}, \mathbf{V}, \pi)$  {Sorted tokens}
  - 3: Pad each group to  $\max_k |\mathcal{G}_k|$ ; reshape to  $(BK, \max_k |\mathcal{G}_k|, H, d)$
  - 4:  $\mathbf{o}_A, \ell_A \leftarrow \text{flash\_attn}(\mathbf{Q}_s, \mathbf{K}_s, \mathbf{V}_s, \text{causal=True})$  {Set  $\mathcal{A}$ }
  - 5: Extract real tokens from  $\mathbf{o}_A, \ell_A$ ; unsort via  $\pi^{-1}$
  - 6:  $\mathbf{o}_B, \ell_B \leftarrow \text{cross\_group\_local}(\mathbf{Q}, \mathbf{K}, \mathbf{V}, g, w)$  {Set  $\mathcal{B}$ }
  - 7:  $\mathbf{o} \leftarrow \text{lse\_merge}(\mathbf{o}_A, \ell_A, \mathbf{o}_B, \ell_B)$  {Equation 20}
  - 8: **return**  $\mathbf{o}$
- 

The complete implementation is 320 lines of Python using only `flash_attn_func` and standard PyTorch operations. No custom CUDA kernels, no Triton, no compilation.

## E.4.8 THE SOFT-TO-HARD TRAINING GAP

The fast inference kernel is exact given hard group assignments. The remaining challenge is that our training uses *soft gating*, creating a mismatch between training and inference.

**Training mode.** During training, each pair  $(i, j)$  receives a continuous gate:

$$\text{gate}(i, j) = \sigma\left(\lambda \cdot (\mathbf{g}_i^\top \mathbf{g}_j - 0.5)\right) \quad (22)$$

where  $\mathbf{g}_i$  is the Sinkhorn-normalized group probability of token  $i$ . The gate is applied as  $\log(\text{gate})$  added to attention scores before softmax. Local pairs ( $|i - j| \leq w$ ) receive gate = 1 regardless of group membership.

**Inference mode.** The fast kernel uses top- $k$  group membership: each token  $i$  belongs to its  $k$  highest-scoring groups from  $\mathbf{g}_i$ . Two distant tokens attend only if they share  $\geq 1$  group; otherwise gate = 0 (excluded from attention). The special case  $k=1$  is argmax.

**The mismatch.** During soft-gated training, cross-group distant pairs receive gate values in  $(0, 1)$ —not exactly zero. The model learns to use this signal: empirically, cross-group distant pairs account for  $\sim 3.5\%$  of total attention mass at layer 0, weighted by a mean gate of  $\sim 0.72$ . At inference, this 3.5% is zeroed out.

The per-layer error is small: cosine similarity between soft-gated and hard-assigned outputs is 0.9978 at a single layer. But the error *compounds* across 12 layers—each layer’s output feeds the next layer’s input. On GPT-2 124M / PG-19:

Mode	PPL	$\Delta$
Soft gating (training)	85.1	—
Hard assignment (fast)	122.5	+37.4

**Why standard fixes fail.**

- **High  $\lambda$ :** Increasing  $\lambda$  to make gates binary pushes *all* gates toward 1.0 (not toward 0 or 1), because the affinity  $\mathbf{g}_i^\top \mathbf{g}_j$  is always positive after Sinkhorn normalization. The centered formula  $\sigma(\lambda \cdot (a - 0.5))$  fixes the floor but high  $\lambda$  causes vanishing gradients:  $\sigma'(x) \approx 0$  when  $|x| \gg 0$ , preventing centroid learning.
- **$\lambda$  annealing:** Start with low  $\lambda$  (good gradients, soft gates), gradually increase to high  $\lambda$  (binary gates, weak gradients). This is the most promising direction—the model learns group structure while gates are soft, then hardens them after centroids have converged.
- **Gumbel-softmax:** Replace soft group assignment with Gumbel-softmax sampling, which is differentiable but produces hard one-hot assignments in the forward pass. This would make training match inference exactly.

**$\lambda$  annealing reduces the argmax gap.** The fast inference kernel is mathematically exact (cosine similarity 1.0000 against reference). Preliminary experiments with  $\lambda$  annealing ( $\lambda: 2 \rightarrow 12$  over 8000 steps with 50% warmup) reduce the argmax gap from +87.6 PPL (no annealing) to +6.6 PPL—a 13 $\times$  reduction (Table 28).

Method	Soft PPL	Hard PPL	Gap
Fixed $\lambda=2$ (no annealing)	41.9	129.4	+87.6
Annealing $\lambda: 2 \rightarrow 20$ , 8K steps	39.9	55.0	+15.1
Annealing $\lambda: 3 \rightarrow 15$ , 10K steps	40.2	46.2	+6.0
Annealing $\lambda: 2 \rightarrow 12$ , 8K steps	40.3	46.9	+6.6

Table 28:  $\lambda$  annealing reduces the argmax ( $k=1$ ) gap.  $\lambda_{\text{end}} \in [12, 15]$  with 50% warmup provides the best tradeoff.

**Top- $k$  membership eliminates the gap.** The residual  $\sim 6$  PPL gap from  $\lambda$  annealing arises because argmax ( $k=1$ ) forces each token into exactly one group, losing genuinely useful cross-group connections. Top- $k$  group membership (Section 3.2) resolves this without any change to training: at  $k=2$  with  $K=4$  groups, each token belongs to its two highest-scoring groups, retaining  $\sim 60\%$  of attention pairs.

The result is striking: top- $k=2$  achieves 41.3 PPL (5K training steps)—*better* than both soft-gated training (42.9) and the pretrained model (42.8)—at  $2\times$  speedup. With extended training (20K steps), soft PPL improves to 41.0 and argmax improves to 74.0 (from 82.9), while top- $k=2$  remains at 42.2—still below pretrained. The argmax gap is not merely closed but *inverted*: discrete routing with  $k=2$  surpasses continuous gating.

Interestingly, shorter training produces *better* top- $k=2$  results (41.3 at 5K vs. 42.2 at 20K) because softer assignments (confidence 0.89 vs. 0.94) yield more selective pruning: top- $k=2$  retains 60% of pairs at 5K vs. 74% at 20K. This suggests an optimal assignment sharpness for each  $k$ —a direction we leave to future work.

This reframes the soft-to-hard problem. The gap was never about soft vs. hard assignment per se, but about the granularity of discretization. Argmax is too coarse: it discards useful cross-group connections. Top- $k=2$  is the right discretization—sparse enough for  $2\times$  speedup, inclusive enough to retain the connections that matter. The learned centroids identify which connections are signal and which are noise;  $k=2$  membership lets the inference kernel act on this knowledge.

#### E.4.9 REMAINING OPEN QUESTION: TRAINING-TIME SPEEDUP

Top- $k$  membership resolves the inference gap but not the training cost: soft-gated training still computes all  $O(n^2)$  pairs. Training directly with discrete group assignment (for training-time efficiency) remains open. Straight-through estimators and Gumbel-softmax are natural candidates but face gradient quality challenges with the small centroid-only parameter budget ( $\sim 7\text{M}$  parameters). We leave this to future work.